

Response to Referee 1

M. Angeles Gallego, Axel Timmermann, Tobias Friedrich, Richard E. Zeebe

July 17, 2018

We thank the referee for reviewing the manuscript and for giving insightful and detailed comments that helped to improve our manuscript noticeably.

Comment 1:

The changing seasonality in the surface ocean $p\text{CO}_2$ and its potential impact on ocean acidification and marine life has recently received a lot of attention. More and more evidence emerges that the excess uptake of CO_2 by the oceans will lead to environmental stress conditions, which will emerge earlier in time due to the seasonal $p\text{CO}_2$ and pH amplification. The authors present here an extensive analysis building on state-of-the-art modeling output to estimate how strong the CO_2 amplification is expected to be by the end of the century and what the main drivers of this amplification are. In my view, one strength of the conducted analysis is, that it nicely bridges between 2 recently published studies by Landschützer et al. (2018) and Kwiatkowski and Orr (2018) (both cited in the main text), hence I do believe the study has its place in the current literature and the results will be of interest to experts and the wider BG readership.

Unfortunately, while bridging between the current literature is the strong point of the presented manuscript, it also reveals its strongest weakness. On many occasions the authors fail to clearly highlight what is novel about their analysis and what has been previously shown. While the authors do give credit e.g. to the Landschützer et al. (2018) and Kwiatkowski and Orr (2018) studies at some place in the text (hence they must have read them), they fail to discuss their results in context to what is already known by these other studies. In some cases, the authors even create the impression that conclusions drawn here are novel, whereas they have been highlighted in other studies. To name the concrete examples:

Response: We revised large part of the manuscript to properly identify which findings are novel and which ones already exists in the current literature.

We added two supplementary figures: Fig. S3 that shows a comparison of

pCO₂ seasonal amplitude by Landschützer et al. (2017) and Takahashi et al. (2014), as well as their thermal and non-thermal components. Fig. S4 shows a comparison of summer-minus-winter pCO₂ amplitude between models, for 2006-2026 and 2080-2100 periods.

Below we address the specific referee's comments. Subsequently, we list other changes that were made to the manuscript, as well as references added.

Comment 2: Page 6 lines 1-2: "In general, towards the end of the century pCO₂ amplifies more in high latitudes, . . .". This is the same result as for the past years based on observational data ((Landschützer et al., 2018), Figure 4) and for the future pH as a direct consequence of CO₂ ((Kwiatkowski and Orr, 2018), Figure 3)).

Response: We changed the sentence to: " In general, towards the end of the century the pCO₂ amplifies more in high latitudes, but so does the standard deviation uncertainty among models. This regional pattern agrees with the observation-based findings of Landschützer et al. (2018) which show that high latitudes have already experienced a larger amplification than mid-low latitudes from 1982 to 2015. Furthermore, the same pattern is projected by CMIP5 models for the seasonal amplification of [H⁺] by the end of the century (Kwiatkowski and Orr, 2018). This is expected from the near-linear relation between pCO₂ and [H⁺]."

Comment 3: Page 9 lines 6-7: "We demonstrate that on average the global amplification of pCO₂ is due to the overall longterm increase of anthropogenic CO₂". This is the same conclusions Landschützer et al. (2018) reached based on examining trends in amplitude over the past 30 years, yet this is nowhere indicated. It is still a valuable result considering the focus of the study being the coming century, but it needs to be highlighted that other studies derive to the same conclusion.

Response: We changed the sentence to: "In agreement with Landschützer et al. (2018), also the model projections towards the end of this century demonstrate that the global amplification of δ pCO₂ is due to the overall longterm increase of anthropogenic CO₂. A higher oceanic background CO₂ concentration enhances the effect of T-driven solubility changes on δ pCO₂ and alters the seawater carbonate chemistry, also enhancing the DIC seasonality effect. "

Comment 4: Page 9 lines 11-12: "Our results extend and refine the current views, in which the future amplification has been attributed uniquely to the DIC sensitivity". This is not correct. Both Landschützer et al. (2018)and Kwiatkowski and Orr (2018)

discuss the attribution of other terms as well. The authors even briefly mention this in their introduction page 2 line 32: "Current literature suggests that the seasonal amplification is a consequence of an increase on the T and DIC contributions to pCO₂ (Landschützer et al., 2018)..."

Response: We agree, we removed the sentence.

Comment 5: Page 9 lines 17-19: "The first complete analytical Taylor expansion of pCO₂ in terms of the variables DICs, TAs, T and S showed that DICs and T contributions are the main counteracting terms to control the pCO₂, both under present-day and future conditions. The prevalence of one term over the other in various regions remains similar, even under enhanced CO₂ conditions". This has also been shown by Landschützer et al. (2018) under past/present conditions, yet again this is not mentioned anywhere. Furthermore, by stating "The first complete Taylor expansion . . ." I suppose the authors mean within their own study, yet it created the impression that the authors refer to the first complete Taylor expansion overall, whereas, e.g. Kwiatkowski and Orr (2018) use the same Taylor expansion in their analysis.

Response: By "first complete analytical Taylor expansion," we refer to the incorporation of T and S analytical terms, and therefore it is the first complete with analytical expressions in the four terms, which - to our knowledge - has not been done before. However, we agree this might be misleading, so we changed the sentence to: "The models confirm the well-established mechanisms controlling present-day δpCO_2 (Takahashi et al., 2002; Sarmiento and Gruber, 2006; Fay and McKinley, 2017). DIC_s and T contributions are the main counteracting terms dominating the seasonal evolution of δpCO_2 . Furthermore, the models show that under future conditions the controlling mechanisms remain unchanged. This result confirms the findings of Landschützer et al. (2018) that identified the same regional controlling mechanism for the past 30 years. The relative role of the DIC and T terms is regionally dependent. High latitudes and upwelling regions, such as the California Current system and the coast of Chile, are dominated by DIC_s and the temperate low latitudes are driven by T. Only in the North Atlantic and North-Western Pacific the models show a dominance of thermal effects over non-thermal effects, which is in disagreement with observations. This further illustrates the urgent need for models to accurately represent regional oceanographic features to accurately reproduce the δpCO_2 characteristics." The discussion on the difference between models and observations was added in the results and discussion section.

Comment 6: Page 9 lines 23-26: "Spatially, we found that the magnitude of the contributions depends on the mean $p\text{CO}_2$, its local sensitivities (DIC,TA,T,S) and the amplitude of their seasonal cycles ((DIC,TA,T,S)). The phases depend on the regional characteristics of the seasonal cycles and they moderate the counteracting nature of both contributions. The compensation of DICs and T contributions is most effective when they are six months out of phase." This mirrors again a conclusion drawn in Landschützer et al. (2018) (see e.g. Figure 3 in their study), whereas a comparison, discussion or even mentioning of this circumstance is missing here. Also regional characteristic have been discussed by Landschützer et al. (2018) and in terms of pH by Kwiatkowski and Orr (2018).

Response: The sentence was changed to: "Moreover, the $p\text{CO}_2$ seasonal cycle amplitude depends on the relative magnitude and phase of the contributions. The models ensemble mean reproduces the highly effective compensation of DIC_s and T contributions when they are six months out of phase, confirming previous studies (Takahashi et al., 2002; Landschützer et al., 2018). The compensation of DIC and T prevents a larger amplification of $\delta p\text{CO}_2$, even when both contributions are largely amplified."

Comment 7: Another important result is only "hand wavy" introduced, namely that TA and S play a lesser role in the future $p\text{CO}_2$ cycle amplification. One of the weak points of the Landschützer et al. (2018) study is that the authors ignore e.g. TA contributions, yet this study suggests that is of minor concern even when evaluating the century-long seasonal amplification. The authors also discuss second order terms here that have not been introduced in Landschützer et al. (2018) or Kwiatkowski and Orr (2018), but this is also not mentioned/compared.

Response: We added in the conclusions, page 11, line 6: "The amplification of the TA and S contributions have a small impact on $\delta p\text{CO}_2$ in most regions, except in the high latitudes where the TA contribution complements the DIC one, enhancing the non-thermal effect in this region." We added in the results section, page 10, line 5: "In general, the $\Delta\delta T$ contribution gains importance as we move poleward in both hemispheres and therefore the second order terms originating from $\Delta\overline{p\text{CO}_2} \cdot \Delta\delta T$ also reinforce the amplification. Interestingly, in the high latitudes, the amplification through second order terms is as important as the change in the seasonality of the drivers."

Comment 8: Very interesting regional differences occur between the observation-based assessment of Landschützer et al. (2018) and this study, that are not discussed at all. Landschützer

et al. (2018) find a DIC dominance in the high latitudes of both hemispheres, whereas the model based study suggests a T dominated increase in the high latitude northern hemisphere. Is this due to a model bias in seasonality. Is this the same across all models?.

Response: We added in the "Results and discussion" section, page 7, line 2: "The models show that the $\delta p\text{CO}_2$ in the 40°N to 60°N band is controlled by T, which disagrees with the above mentioned observations that show a non-temperature dominance in this band. The difference between models and observations arises from two regions: the North Atlantic basin and the North Western Pacific; specifically near the Oyashio Current, and the outflows from the Okhotsk Seas (see Supplementary Fig. S3). Most models show a T dominance in the North Atlantic basin; only CESM1-BGC and GFDL-ESM2M show a DIC dominance (see Supplementary Fig. S4). The North Atlantic is one of the major sinks of anthropogenic CO_2 , however some models fail to estimate its uptake capacity (Goris et al., 2018). Goris et al. (2018) found that models with an efficient carbon sequestration present a DIC-dominated $p\text{CO}_2$ seasonal cycle in the North Atlantic, but models with low anthropogenic uptake show a T dominance in this region. In the North-Western Pacific, Mckinley et al. (2006) found that coarse models are not able to capture the intricate oceanographic features of this area, and therefore the $p\text{CO}_2$ seasonality is not well captured."

Comment 9: The authors have conducted an extensive, interesting and certainly valuable analysis using state-of-the-art model outputs. Their methods are sound and their results nicely fit alongside the existing literature. The lack of discussion with the existing literature, however, is of major concern, particularly that the authors fail to acknowledge similar studies coming to the same conclusions. If the authors were to revise their manuscript and discuss their results in a fair way considering the existing literature, I believe this study can be considered for publication. The revisions however will affect the text throughout, hence I recommend major revisions of the manuscript.

Response: As suggested by the referee, we have done a major revision of the manuscript. We thank again for the suggestions that helped to improve the manuscript; we placed our results and their relevance among the current literature and compared/contrasted our findings with previous results, in particular those by Landschützer et al. (2018).

Comment 10: Abstract line 1: "observations" its observation-based

Response: Changed to "observation-based results"

Comment 11: Introduction page 1 line 22: a third of the anthropogenic CO₂ produced by fossil fuel burning, cement production and deforestation since the industrial revolution". The cited Sabine study suggest 48% since the beginning of industrialization. The referenced 1/3 refer to the annual uptake as stated in the second study cited, namely the Le Quere et al carbon budget.

Response: We changed it to: "the ocean has absorbed nearly half of the anthropogenic CO₂ produced by fossil fuel burning and cement production since the industrial revolution (Sabine et al., 2004)"

Comment 12: Page 2 line 21: [CO₂(aq)] is introduced. For the non carbonate seawater chemists that read BG it would be helpful to explain the difference between [CO₂] and [CO₂(aq)]

Response: We changed it to: " This is due to the ability of CO₂ to react with seawater to form bicarbonate [HCO₃⁻] and carbonate [CO₃²⁻], leaving only a small portion of the dissolved carbon dioxide in the form of aqueous CO₂ ([CO₂(aq)]). [CO₂(aq)] together with the carbonic acid ([H₂CO₃]) are defined as [CO₂]. Therefore, it is useful to define the total amount of carbon as DIC, which is the sum of the three carbon species ([HCO₃⁻], [CO₃²⁻] and [CO₂])."

Comment 13: Page 4 line 11 and Supplement figure S1: The comparison between individual models gets worse in the high latitudes. Any idea why? The high latitude northern hemisphere is also where this study differs from the observation-based analysis of Landschützer et al. (2018).

Response: In this figure we compare the pCO₂ amplification calculated as model output with the value from the Taylor expansion. The Taylor expansion is less precise in higher latitudes, probably because second order terms gain importance. The difference with Landschützer et al. (2018) was addressed in comment 8.

Comment 14: Page 4 line 20, equation 3 and following: the delta terms also represent the mean seasonal cycle over 20 years (period 1 or period 2) hence they should have also an overbar (like the pCO₂) for consistency.

Response: We leave the nomenclature as it is, as by "mean" we refer to the mean value of the data, instead of the deviation of the mean, which is

the seasonal cycle.

Comment 15: Page 5 line 14: "The range agrees with previous estimates by Takahashi et al. (2002)." Please add the comparison (visual or in table form), e.g. in the supplement for the readers of this study. Otherwise the reader has to jump around several different manuscripts for a simple comparison.

Response: We added a supplementary figure S3, for better comparison with data from Takahashi et al. (2014), for a reference year 2005 and with Landschützer et al. (2017). We also added at page 5, after line 14 : "The ensemble mean initial seasonal amplitude range is in good agreement with observational estimates calculated for the reference year 2005 (Takahashi et al., 2014), and for the 1982-2015 period (Landschützer et al., 2017). The agreement between models and observations is remarkably good in the equatorial regions, but the initial amplitude is slightly overestimated in the mid and high latitudes (see Supplementary Fig. S3).The higher amplitude in models than observations is expected, as the initial period 2006-2026 already experienced an amplification compared to previous years. Moreover, Tjiputra et al. (2014) found that the ocean's pCO₂ historical trend is larger in models than observations when it is estimated in large scale areas of the ocean. However, they found that models' pCO₂ trends agree with observations when the trends are subsampled to the locations where the observations were taken, and therefore they do a good job reproducing well-known time series. Moreover, differences are expected as Pilcher et al. (2015) suggested that CMIP5 models perform well in reproducing the seasonal cycle timing, but still show considerable errors in reproducing the seasonal amplitude of pCO₂ due to differences in the mechanisms represented in each model, especially in subpolar biomes. "

Comment 16: Page 5 line 21: "Our mean amplification factor estimation agrees with the lower end range of McNeil and Sasse (2016)." Please add numbers for the reader of this study.

Response: We changed this sentence to: " Our mean amplification factor estimation agrees with the threefold amplification found for most of the ocean by McNeil and Sasse (2016)."

Comment 17: Page 6 lines 8-9: "Our estimated contributions from DICs and T to the present day pCO₂ are in good agreement with the data based estimates (Takahashi et al., 2002; Fay and McKinley, 2017)." Please add a visual comparison or numbers for the readers of this study.

Response: Instead of comparing with Takahashi et al. (2002), and Fay and McKinley (2017), we used the dataset of Takahashi et al. (2014) and calculated thermal and non thermal components for year 2005. We also added a comparison with the thermal and non-thermal components for years 1982-2015 that Peter Landschützer kindly provided to us. The results are shown in Supplementary Figure S3, and the discussion was added in section 3.2: "For most of the ocean, the ensemble mean estimated contributions from DIC_s and T to the present-day δpCO_2 are in good agreement with the data-based estimates of Takahashi et al. (2014) and Landschützer et al. (2017), particularly in the equatorial regions (see Supplementary Fig. S3). However our T and DIC contributions are slightly larger in mid and high latitudes, for the same reasons the pCO_2 seasonal amplitude is overestimated (see Section 3.1). Also, differences arise between our DIC_s contribution and the observation-based so called "non-thermal" contribution, because the non-thermal contribution also includes the total alkalinity and salinity effects. Nonetheless, between 40°S - 40°N our ensemble mean shows that δpCO_2 is dominated by changes in temperature that control CO_2 solubility, which decreases in summer enhancing pCO_2 , in agreement with observations. The Southern Ocean is controlled by DIC, that responds to changes in upwelling and phytoplankton blooms. Both mechanisms act together to decrease (increase) DIC in summer (winter) (Sarmiento and Gruber, 2006)." The discussion of northern high latitudes is added in comment 8.

Comment 18: Page 7 lines 6-7: "DIC must not be confused with the Revelle factor, which is defined as $R = \text{DIC} \times \gamma_{\text{DIC}}$ ". This statement comes a bit out of the blue and while true it is not clear to me why it appears here. Based on the equations/wording used in this study I don't see the danger that these terms are mixed up.

Response: The Revelle factor and the sensitivity are different, and sometimes confused. We included the relationship because Takahashi et al. (1993) computed the Revelle factor. This sentence was rearranged as: "This follows the approach of Takahashi et al. (1993), however instead of computing the Revelle factor we use γ_{DIC} , both terms are related by $R = \text{DIC} \cdot \gamma_{\text{DIC}}$."

Other changes added:

- page 7, line 25 we added: " In this region some models underestimate the pCO_2 trend (Tjiputra et al., 2014), and therefore the seasonal amplification might be underestimated too."
- page 7, line 32, we added: "Lower buffer factors (higher sensitivities factors) are found in regions where DIC and TA have similar values,

and they will decrease (increase) as the DIC/TA ratio in the oceans increases (Eggleston et al., 2010). ”

- page 8, line 3, we added: ” $\gamma_{S_{fw}}$ decreases everywhere except in the Western Pacific Warm Pool. In this region $\gamma_{S_{fw}}$ increases probably due future changes in precipitation that enhance the fresh-water effect.”
- page 9, line 5 was changed to: ”Kwiatkowski and Orr (2018) demonstrated that the seasonality of the drivers is important to determine future changes in $[H^+]$ seasonality. In the same fashion, our results show that the four δpCO_2 drivers present changes in seasonality, and in particular δDIC_s and δT changes are important to explain future projections of the δpCO_2 amplitude.”

References

- Eggleston, E. S., Sabine, C. L., and Morel, F. M. M.: Revelle revisited: Buffer factors that quantify the response of ocean chemistry to changes in DIC and alkalinity, *Global Biogeochem. Cycles*, 24, GB1002, 2010.
- Fay, A. R. and McKinley, G. A.: Correlations of surface ocean pCO_2 to satellite chlorophyll on monthly to interannual timescales, *Global Biogeochem. Cycles*, 31, 436–455, 2017.
- Goris, N., Tjiputra, J., Olsen, A., Schwinger, J., Lauvset, S. K., and Jeansson, E.: Constraining projection-based estimates of the future North Atlantic carbon uptake, *Journal of Climate*, 31(10), 3959–3978, 2018.
- Kwiatkowski, L. and Orr, J.: Diverging seasonal extremes for ocean acidification during the twenty-first century, *Nat. Clim. Change*, 8, 141–145, 2018.
- Landschützer, P., Gruber, N., and Bakker, D.: An updated observation-based global monthly gridded sea surface pCO_2 and air-sea CO_2 flux product from 1982 through 2015 and its monthly climatology (NCEI Accession 0160558). Version 2.2. NOAA National Centers for Environmental Information. Dataset. doi:10.7289/V5Z899N6, 2017.
- Landschützer, P., Gruber, N., Bakker, D. C. E., Stemmler, I., and Six, K. D.: Strengthening seasonal marine CO_2 variations due to increasing atmospheric CO_2 , *Nat. Clim. Change*, 8, 146–150, 2018.
- McKinley, G. A., Takahashi, T., Buitenhuis, E., Chai, F., Christian, J. R., Doney, S. C., Jiang, M., Lindsay, K., Moore, J. K., Quere, C. L., Lima, I., Murtugudde, R., Shi, L., and Wetzel, P.: North Pacific carbon cycle response to climate variability on seasonal to decadal timescales, *J. Geophys. Res.*, 111, C07S06, 2006.

- McNeil, B. I. and Sasse, T. P.: Future ocean hypercapnia driven by anthropogenic amplification of the natural CO₂ cycle, *Nature*, 529, 383–386, 2016.
- Pilcher, D. J., Brody, S. R., Johnson, L., and Bronselaer, B.: Assessing the abilities of CMIP5 models to represent the seasonal cycle of surface ocean pCO₂, *J. Geophys. Res. Oceans*, 120, 4625–4637, 2015.
- Sabine, C. L., Feely, R. A., Gruber, N., Key, R. M., Lee, K., Bullister, J. L., Wanninkhof, R., Wong, C., Wallace, D. W. R., Tilbrook, B., Millero, F. J., Peng, T. H., Kozyr, A., Ono, T., and Rios, A. F.: The oceanic sink for anthropogenic CO₂, *Science*, 305, 367–371, 2004.
- Sarmiento, J. L. and Gruber, N.: *Ocean Biogeochemical Dynamics*, Princeton University Press, Princeton, New Jersey, USA, 2006.
- Takahashi, T., Olafsson, J., Goddard, J. G., Chipman, D. W., and Sutherland, S. C.: Seasonal variation of CO₂ and nutrients in the high-latitude surface oceans: A comparative study, *Global Biogeochem. Cycles*, 7, 843–878, 1993.
- Takahashi, T., Sutherland, S. C., Sweeney, C., Poisson, A., Metzl, N., Tilbrook, B., Bates, N., Wanninkhof, R., Feely, R. A., Sabine, C. L., Olafsson, J., and Nojiri, Y.: Global sea-air CO₂ flux based on climatological surface ocean pCO₂, and seasonal biological and temperature effects, *Deep-Sea Research II*, 49, 1601–1623, 2002.
- Takahashi, T., Sutherland, S. C., Chipman, D. W., Goddard, J. G., Newberger, T., and Sweeney, C.: Climatological Distributions of pH, pCO₂, Total CO₂, Alkalinity, and CaCO₃ Saturation in the Global Surface Ocean. ORNL/CDIAC-160, NDP-094. Carbon Dioxide Information Analysis Center, <https://doi.org/10.3334/CDIAC/OTG.NDP094>, 2014.
- Tjiputra, J. F., Olsen, A. R. E., Bopp, L., Lenton, A., Pfeil, B., Roy, T., Segschneider, J., Totterdell, I. A. N., and Heinze, C.: Long-term surface pCO₂ trends from observations and models, *Tellus B*, 66, 23 083, 2014.

Response to Referee 2

M. Angeles Gallego, Axel Timmermann, Tobias Friedrich, Richard E. Zeebe

July 17, 2018

We are thankful for the referee's comments. The referee's specific comments helped with the revision of our calculations and improved the manuscript.

Comment 1: In this study, the authors assess future changes in the seasonal cycle of surface ocean pCO₂ using simulations from 7 different CMIP5 Earth system models subjected to RCP8.5 forcing. A Taylor series decomposition approach is used to identify the important drivers of pCO₂ seasonality and its future changes. The authors find that the pCO₂ seasonal amplitude will increase by a factor of 1.5 to 3 by the end of the current century. The primary cause of this increase is the increase in ocean mean pCO₂ (a response to increasing anthropogenic emissions), which enhances the pCO₂ seasonal variation occurring in response to seasonal variations in temperature (T) and dissolved inorganic carbon (DIC). Changes in T and DIC seasonality at high latitudes are also relevant for understanding the model-simulated changes in pCO₂ seasonality. This is a nice study that complements some recent work (e.g., McNeil and Sasse (2016); Landschützer et al. (2018); Kwiatkowski and Orr (2018)) examining the changing seasonality of ocean carbonate chemistry variables over recent decades and in the future. The paper is generally clear, well written and logically organized, and the scientific methods are sound. However, I do strongly agree with Referee 1's assessment that the authors should do a better job of placing their results in the context of previous work. While this is done to some extent already and, in all fairness, the authors certainly cite the relevant literature it tends to get a bit lost in the discussion and it's often a little unclear which results are novel and which simply confirm previous findings. It could be helpful to add a separate Discussion section before the Summary and Conclusions in which results from the current study are compared and contrasted with those from previous studies. In addition to this, I've included several specific comments and technical corrections below for the authors to consider. I feel that a suitably revised version of the manuscript - addressing the points raised here - should be publishable in Biogeosciences.

Response: We revised the "Results and discussion" section, where we compared and contrasted our results with the existing literature. We added several changes in this section based on referee 1 and 2 comments. Most of the changes were discussed in the response to referee's 1 comments. In what follows we address referee 2's specific comments:

Comment 2: p. 5, lines 19-20: "McNeil and Sasse (2016) using a data-based approach" It would be good to clarify what you mean here by a "data-based approach".

Response: We changed to "McNeil and Sasse (2016) used observations and a neural-network-clustering algorithm to project that by year 2100..."

Comment 3: p. 5, lines 23-25: "Using observations Landschützer et al. (2018) found..." I have two issues with this sentence. First, it's unclear to me where the mean 20 μatm increase by the end of the century comes from; the values given earlier in this paragraph (see also Fig. 1) are significantly larger than this (e.g., 41 μatm increase between 40S-40N). Second, I wouldn't expect the rate of change of pCO_2 seasonality in observations to match that in the CMIP5 models in the RCP8.5 simulations, since many of the important drivers of pCO_2 variability (e.g., atmospheric CO_2) are changing at much faster rates in the latter than they are in the former.

Response: We did three changes based on this comment: We corrected the calculation and the sentence was changed to: "Using observations, Landschützer et al. (2018) found an increase of 2.2 μatm per decade, which is smaller than our findings of a total 42 μatm increase by the end of the century between 40°S-40°N, and a global-mean change of 81 μatm on the high latitudes. This difference is again possibly due the higher mean pCO_2 values in models than observations." The discussion of the difference between models and observations was addressed in the response to Referee 1, Comment 15.

Comment 4: Fig. 3/Fig. S1: These figures show (among other things) that the Taylor expansion generally does a good job in reproducing the actual pCO_2 calculated from model output. However, there seems to be an inconsistency between the two figures. Specifically, Fig.3 suggests that the Taylor expansion slightly overestimates the seasonal amplitude of pCO_2 (this is most evident for the 40S-70S latitude band), while Fig. S1 suggests exactly the opposite: an underestimation of the seasonal amplitude.

Response: The labels of the S1 figure's axis were switched (x-axis label was y-axis, and vice versa). Figure S1 was corrected.

Comment 5: p. 7, line 15: "decrease in the future to a global mean value of 0.035" .This number seems to be too small looking at Fig. 4c (middle column).

Response: There was an error in the calculation. The sentence was changed to: "This value agrees with our global mean ensemble estimate of 0.0428. However, our analytical expression of γ_T shows that this value varies regionally and, by reasons unknown to us, it might decrease in the future to a global mean value of 0.0415, (Fig. 4, row (c), third column). "

Comment 6: p. 7, line 26: "with lower temperatures in winter and higher in summer" It might be good to clarify here that you do not mean lower temperatures in an absolute sense (i.e., winter temperatures are certainly projected to be higher at the end of century under RCP8.5 than they are at present).

Response: This sentence was changed and we added the proper context: "All models show a slight increase in δT , only one model showed a slightly decrease in the southern region, and two models showed a decrease in the equatorial region during October to December. It is important to note that Fig. 5 shows the seasonal values, with the mean T removed. Therefore, when considering the positive T trends, the absolute summer values show an increase and the absolute winter values a decrease. This agrees with the results of Alexander et al. (2018); who showed that models project a seasonal intensification of T, with larger warm extremes and reduced cold extremes. The authors attributed the T seasonality intensification to an increased oceanic stratification and an overall shoaling of the mixed layer depth, which confines seasonal changes in a reduced volume of water, producing larger changes at the surface. They also showed that the intensification trends are stronger in summer than winter, as the mixed layer depth is shallower in summer. Moreover, ice covered regions will experience the largest increase in T seasonality due the loss of sea ice, because the ice melting/freezing moderates the surface water temperature seasonality(Carton et al., 2015). "

Comment 7: p. 8, lines 26-27: "we decomposed the DICs and T contributions..." I only see the seasonal cycle and mean $p\text{CO}_2$ components in Fig. 6b, not the sensitivity component.

Response: We changed the sentence to: "To further disentangle which of the two main drivers (DIC_s or T) is most affected by $\Delta \overline{p\text{CO}_2}$, we decomposed the DIC_s and T contributions in their sensitivity, seasonal cycle and $\overline{p\text{CO}_2}$ components. Figure 6, (b), shows the total DIC and T components

together with the $\Delta\overline{pCO_2}$ and seasonal cycles effects on them. The effects from the sensitivities are not depicted, as they only play a minor role. Only the $\Delta\gamma_{DIC}$ term gains importance in the Southern Ocean (not shown). ”

Comment 8: Technical corrections: 1) p. 1, line 2: Should be a rate of 2-3 μatm per decade?.

Changed to decade.

2) p. 3, line 5: ”Methodology” misspelled.

Corrected.

3) p. 3, line 14: Should be scarce?.

Changed to ”scarced”.

4) p. 7, line 11: Should probably remove the word ”change” here, since the annual cycle amplitude change is actually 168 μatm minus 96 μatm (i.e., 72 μatm).

We removed the word ”change” and changed the sentence to: ”therefore, for a $\overline{pCO_2}$ equal to 800 μatm , the δpCO_2 amplitude due to δDIC amounts to 168 μatm . ”

5) p. 7, line 15: Should be ”row (c)”.

Changed to ”row c)”

References

- Alexander, M. A., Scott, J. D., Friedland, K. D., Mills, K. E., Nye, J., Pershing, A. J., and Thomas, A. C.: Projected sea surface temperatures over the 21st century: Changes in the mean, variability and extremes for large marine ecosystem regions of Northern Oceans, *Elem. Sci. Anth.*, 6, 9, 2018.
- Carton, J. A., Ding, Y., and Arrigo, K. R.: The seasonal cycle of the Arctic Ocean under climate change, *Geophys. Res. Lett.*, 42, 7681–7686, 2015.
- Kwiatkowski, L. and Orr, J.: Diverging seasonal extremes for ocean acidification during the twenty-first century, *Nat. Clim. Change*, 8, 141–145, 2018.
- Landschützer, P., Gruber, N., Bakker, D. C. E., Stemmler, I., and Six, K. D.: Strengthening seasonal marine CO_2 variations due to increasing atmospheric CO_2 , *Nat. Clim. Change*, 8, 146–150, 2018.
- McNeil, B. I. and Sasse, T. P.: Future ocean hypercapnia driven by anthropogenic amplification of the natural CO_2 cycle, *Nature*, 529, 383–386, 2016.

Drivers of future seasonal cycle changes of oceanic pCO₂

M. Angeles Gallego¹, Axel Timmermann^{2,3,4}, Tobias Friedrich², and Richard E. Zeebe¹

¹Department of Oceanography, School of Ocean and Earth Sciences and Technology, University of Hawaii at Manoa, Honolulu, Hawaii, USA

²International Pacific Research Center, School of Ocean and Earth Sciences and Technology, University of Hawaii at Manoa, Honolulu, Hawaii, USA

³Center for Climate Physics, Institute for Basic Science (IBS), Busan, South Korea

⁴Pusan National University, Busan, South Korea

Correspondence: Angeles Gallego(mdla@hawaii.edu)

Abstract. Recent ~~observations~~ observation-based results show that the seasonal amplitude of surface ocean partial pressure of CO₂ (pCO₂) has been increasing on average at a rate of 2-3 μatm per ~~year~~ decade (Landschützer et al., 2018). Future increases of pCO₂ seasonality are expected, as marine CO₂ will increase in response to increasing anthropogenic carbon emissions (McNeil and Sasse, 2016). Here we use 7 different global coupled atmosphere/ocean/carbon cycle/ecosystem model simulations, conducted as part of the Coupled Model Intercomparison Project Phase 5 (CMIP5), to study future projections of the pCO₂ annual cycle amplitude and to elucidate the causes of its amplification. We find, that for the RCP8.5 emission scenario the seasonal amplitude (climatological maximum-minus-minimum) of upper ocean pCO₂ will increase by a factor of 1.5 to 3 times over the next 60-80 years. To understand the drivers and mechanisms that control the pCO₂ seasonal amplification we develop a complete analytical Taylor expansion of pCO₂ seasonality in terms of its four drivers: dissolved inorganic carbon (DIC), total alkalinity (TA), temperature (T) and salinity (S). Using this linear approximation we show that the DIC and T terms are the dominant contributors to the total change in pCO₂ seasonality. ~~At~~ To first order, their future intensification can be traced back to a doubling of the annual mean pCO₂, which enhances DIC and alters the ocean carbonate chemistry. Regional differences in the projected seasonal cycle amplitude are generated by spatially varying sensitivity terms. The subtropical and equatorial regions (40°S-40°N), will experience a $\approx 30\text{-}80\mu\text{atm}$ increase in seasonal cycle amplitude almost exclusively due a larger background CO₂ concentration that amplifies the T seasonal effect on solubility. This mechanism is further reinforced by an overall increase in the seasonal cycle of T, as a result of stronger ocean stratification and a projected shoaling of mean mixed layer depths. The Southern Ocean will experience a seasonal cycle amplification of $\approx 90\text{-}120\mu\text{atm}$ in response to the mean pCO₂-driven change of the mean DIC contribution and to a lesser extent to the T contribution. However, a decrease of the DIC seasonal cycle amplitude somewhat counteracts this regional amplification mechanism.

20 1 Introduction

Owing to its large ~~buffering capacity, or~~ chemical capacity to resist changes in CO₂ concentration ([CO₂]) (referred to as buffering capacity), the ocean has absorbed nearly a third-half of the anthropogenic CO₂ produced by fossil fuel burning ; ~~cement production and deforestation and cement production~~ since the industrial revolution (Sabine et al., 2004; Le Quéré et al., 2015)

(Sabine et al., 2004). While the ocean's absorption of CO₂ lowers the atmospheric concentration, it also increases the ocean's [CO₂] and in turn lowers its buffering capacity. This leads to a reduction in the oceanic uptake of CO₂ and an intensification of the pCO₂ seasonal cycle (from now on referred to as δpCO_2) (McNeil and Sasse, 2016; Völker et al., 2002). In a recent observational study (Landschützer et al., 2018) key observational study by Landschützer et al. (2018), it was demonstrated that

5 the δpCO_2 is currently increasing amplitude has increased at a rate of $\approx 2\text{-}3 \mu\text{atm}$ per decade, from 1982 to 2015. The pCO₂ already experiences large seasonal fluctuations, which in some regions can reach up to 60% above and below the annual mean pCO₂, (Takahashi et al., 2002). An intensification of the δpCO_2 amplitude could produce seasonal hypercapnia conditions (McNeil and Sasse, 2016) which, together with increased [H⁺] seasonality (Kwiatkowski and Orr, 2018; Hagens and Middelburg, 2016) and aragonite undersaturation events (Hauri et al., 2015; Sasse et al., 2015; Shaw et al., 2013) could

10 expose marine life to harmful seawater conditions earlier than expected if considering only annual mean values. Moreover, a projected amplification of δpCO_2 might increase the net CO₂ uptake in some regions, such as the Southern Ocean, thereby further accelerating the decrease of the buffering capacity in that region (Hauck and Völker, 2015).

The pCO₂ seasonal amplitude is controlled mainly by the seasonal changes in temperature (T) and biological activity ; that usually together with upwelling changes that alter DIC concentrations. Usually, DIC and T changes work in opposite

15 directions (Fay and McKinley, 2017) (Sarmiento and Gruber, 2006; Takahashi et al., 2002; Fay and McKinley, 2017). In subtropical regions higher pCO₂ values occur in summer when solubility decreases. In subpolar regions, pCO₂ increases in winter when waters upwell that are rich in DIC and when respiration of organic matter takes place. Decreased subpolar pCO₂ occurs in summer when the primary productivity is higher and the upwelling diminishes. Therefore, we find close relationships of δpCO_2 with the ocean's [CO₂] that controls the chemical reactions and with the mean pCO₂ that moderates the exchange with

20 the atmosphere. Both factors are related to by the solubility constant that depends on temperature and salinity. Furthermore, the regional differences in the influence of temperature and biology on δpCO_2 are modulated by the ocean's buffering capacity. This is due to the ability of CO₂ to react with seawater to form bicarbonate [HCO₃⁻] and carbonate [CO₃²⁻], leaving only a small portion as of the dissolved carbon dioxide in the form of aqueous CO₂ or ([CO₂(aq)]). [CO₂(aq)] together with the carbonic acid ([H₂CO₃]) are defined as [CO₂]. Therefore, it is useful to define the total amount of carbon as DIC,

25 which is the sum of the three carbon species ([HCO₃⁻], [CO₃²⁻] and [CO₂(aq)]). At current chemical conditions, most of the DIC is in form of HCO₃⁻, therefore the buffering capacity is largely controlled by the CO₃²⁻ capable of transforming CO₂ into bicarbonate through the reaction $CO_2(aq) + CO_3^{2-} + H_2O = 2HCO_3^-$ (Zeebe and Wolf-Gladrow, 2001). The larger the buffering capacity, the larger the pCO₂'s ability to resist changes in DIC. To quantify this capacity, we can introduce the buffer sensitivity factor γ_{DIC} , which is inversely related to the buffering capacity, defined as $\gamma_{DIC} = \partial \ln(pCO_2) / \partial DIC$, (Egleston et al., 2010).

30 Other buffer sensitivity factors are related to the total alkalinity (γ_{TA}), salinity (γ_S) and temperature (γ_T) changes, and are defined in a similar way as $\partial \ln(pCO_2) / \partial TA$, $\partial \ln(pCO_2) / \partial S$ and $\partial \ln(pCO_2) / \partial T$ respectively. It is important to note that the pCO₂ is highly sensitive to temperature due to two factors: first through solubility changes that account for 2/3 of the present day temperature impact, and second, through the dissociation constants that control the carbon system reactions (Sarmiento and Gruber, 2006).

35 While the mechanisms controlling the seasonal cycle of pCO₂ at present day are well documented, the future evolution of

these drivers has not been fully elucidated. Current literature suggests that the seasonal amplification is a consequence of an increase on the T and DIC contributions to $\delta p\text{CO}_2$ (Landschützer et al., 2018) and an increased sensitivity of the ocean to these variables (Fassbender et al., 2017).

The aim of our paper is to provide an in-depth analysis of the mechanisms controlling the future strength of $\delta p\text{CO}_2$ and its regional differences using 7 CMIP5 global earth system models. Our analysis focuses on the 21st century evolution using the Representative Concentration Pathway 8.5 (RCP8.5) scenario. We give a comprehensive analysis of the projected evolution of the DIC, TA, T and S contributions to $p\text{CO}_2$ seasonality. To achieve this goal, we derive explicit analytical expressions for $p\text{CO}_2$ sensitivities in terms of γ_{DIC} , γ_{TA} , γ_{T} and γ_{S} , thereby extending previous work done by Eggleston et al. (2010).

2 Methodology

10 2.1 CMIP5 Models

For our analysis, $p\text{CO}_2$, DIC, TA, T and S monthly-mean output variables covering the period from 2006-2100 were obtained from future climate change simulations conducted with 7 fully coupled earth system models that participated in the Coupled Model Intercomparison Project, Phase 5 (CMIP5). ~~Based on data availability the~~ The following models were selected based on data availability: CanESM2, CESM1-BGC, GFDL-ESM2M, MPI-ESM-LR, MPI-ESM-MR, HadGEM2-ES and HadGEM2-CC (See supplementary material of Hauri et al. (2015)). For the purpose of this paper, we used the Representative Concentration Pathway 8.5 (RCP8.5) future climate change simulations (IPCC, 2013). The ocean's surface data sets were regridded onto a $1^\circ \times 1^\circ$ grid using Climate Data Operators (CDO). The Arctic Ocean and the region poleward of 70°S are removed from the analyses, because observational data for model validation are searescarce.

2.2 Analysis of $\delta p\text{CO}_2$

To elucidate the underlying dynamical, thermodynamical, biological and chemical processes controlling $\delta p\text{CO}_2$ we calculated a first order Taylor series expansion of $\delta p\text{CO}_2$ in terms of its four drivers, DIC, TA, T and S. ~~To verify this approach we compared the sum of the Taylor expansion terms with the full simulated range of $\delta p\text{CO}_2$ from the model's output.~~ While T and S are controlled only by physics, DIC and TA are controlled by physical, chemical and biological processes. Throughout this paper we use salinity-normalized DIC and TA using a mean salinity of 35 psu. This effectively removes the concentration/dilution fresh water effect, following the procedure of Lovenduski et al. (2007). The salinity normalized variables are referred to as DIC_s and TA_s , corresponding to $\text{DIC} \cdot S_0/S$ and $\text{TA} \cdot S_0/S$ respectively. The freshwater effect on DIC and TA is now included in the S term, renamed as S_{fw} . For the Taylor expansion series expansion, each variable ($X=\text{DIC}$, TA, T and S) is decomposed into $X = \bar{X} + \delta X$. The term \bar{X} represents the 21 year-long years-long mean and δX denotes the seasonal cycle (calculated as the monthly mean deviation from the 21 year-years average). The Taylor's expansion is then computed for an initial (2006-2026) and final (2080-2100) period periods. We use multi-decade means and eventually multi-model ensemble means to remove effects of interannual variability. The full first-order series expansion is given by:

$$\delta pCO_2 \approx \frac{\partial pCO_2}{\partial DIC} \Big|_{\frac{T,A,DIC}{T,S}} \delta DIC_s + \frac{\partial pCO_2}{\partial TA} \Big|_{\frac{T,A,DIC}{T,S}} \delta TA_s + \frac{\partial pCO_2}{\partial T} \Big|_{\frac{T,A,DIC}{T,S}} \delta T + \frac{\partial pCO_2}{\partial S} \Big|_{\frac{T,A,DIC}{T,S}} \delta S_{fw} \quad (1)$$

Each term of the right hand side of Eq. (1) represents the contribution from one of the four drivers of δpCO_2 .

5 The analytical expressions for the derivatives (without the salinity normalization) are given by:

$$\begin{aligned} \frac{\partial pCO_2}{\partial TA} \Big|_{\frac{T,A,DIC}{T,S}} &= \overline{pCO_2} \cdot \frac{-\overline{Alk}_c}{DIC \cdot \Theta - \overline{Alk}_c^2} \\ \frac{\partial pCO_2}{\partial DIC} \Big|_{\frac{T,A,DIC}{T,S}} &= \overline{pCO_2} \cdot \frac{\Theta}{DIC \cdot \Theta - \overline{Alk}_c^2} \\ \frac{\partial pCO_2}{\partial T} \Big|_{\frac{T,A,DIC}{T,S}} &= \overline{pCO_2} \cdot \frac{1}{DIC \cdot \Theta - \overline{Alk}_c^2} \left[\overline{TA}_c \cdot \left(\frac{\partial \overline{Alk}_c}{\partial T} + \frac{\partial [B(OH)_4^-]}{\partial T} + \frac{\partial [OH^-]}{\partial T} \right) - \Theta \cdot \frac{\partial (DIC - [CO_2])}{\partial T} \right] - \frac{\overline{pCO_2}}{K_0(T,S)} \cdot \frac{\partial K_0(T,S)}{\partial T} \\ \frac{\partial pCO_2}{\partial S} \Big|_{\frac{T,A,DIC}{T,S}} &= \overline{pCO_2} \cdot \frac{1}{DIC \cdot \Theta - \overline{Alk}_c^2} \left[\overline{Alk}_c \cdot \left(\frac{\partial \overline{Alk}_c}{\partial S} + \frac{\partial [B(OH)_4^-]}{\partial S} + \frac{\partial [OH^-]}{\partial S} \right) - \Theta \cdot \frac{\partial (DIC - [CO_2])}{\partial S} \right] - \frac{\overline{pCO_2}}{K_0(T,S)} \cdot \frac{\partial K_0(T,S)}{\partial S} \end{aligned} \quad (2)$$

10

where $\Theta = [HCO_3^-] + 4[CO_3^{2-}] + \frac{[B(OH)_4^-][H^+]}{(k_b + [H^+])} + [H^+] + [OH^-]$ and $\overline{Alk}_c = [HCO_3^-] + 2[CO_3^{2-}]$. The explicit T and S partial derivatives are given in the Supplementary material (Text S1). The first two derivatives coincide with the results of Egleston et al. (2010) and Hagens and Middelburg (2016), with the exception of the sign of $[OH^-]$ in [their Egleston et al. \(2010\)](#) term S. [To verify this approach we compared the sum of the Taylor expansion terms with the full simulated range of \$\delta pCO_2\$ from the model's output.](#) The Taylor expansion reproduces well the full seasonal cycle amplitude of the original climate model simulations (Supplementary Fig. S1). The analytical expressions for temperature and salinity presented in here are – to our knowledge – the first ones of their kind. Previously the calculation of these terms was based on the approximation given by Takahashi et al. (1993) or on numerical calculations.

20

To gain more insight into the processes causing the amplification of δpCO_2 we introduce a [new-method-method based on a second Taylor series expansion described below](#). Eq. (1) can be rewritten using the expressions for the sensitivities γ determined by the relation $\frac{1}{\overline{pCO_2}} \frac{\partial pCO_2}{\partial X} = \gamma_X$. These sensitivities have been historically used to represent the percentage of change in pCO_2 per unit of DIC, TA, T or S. With this notation, Eq. (1) can be expressed in the following way:

$$25 \quad \delta pCO_2 \approx \overline{pCO_2} \cdot \left(\gamma_{DIC} \cdot \delta DIC_s + \gamma_{TA} \cdot \delta TA_s + \gamma_T \cdot \delta T + \gamma_{S_{fw}} \cdot \delta S_{fw} \right) \quad (3)$$

Each term in Eq.(3) consists of three parts: $\overline{pCO_2}$, the sensitivity γ_X and the corresponding seasonal cycle δX . To understand which component is the main driver for δpCO_2 changes, we perform a second Taylor expansion of the end of the century's δpCO_2 around the initial state of the system in 2006-2026.

To maximize mathematical clarity we will introduce some definitions: first, we introduce the symbol Δ to indicate the difference between the period 2080-2100 and 2006-2026. Therefore, the total future change in $\delta p\text{CO}_2$, is now referred to as $\Delta\delta p\text{CO}_2$. In the same manner, the total change in sensitivities and seasonal cycles are written as $\Delta\gamma_{\text{DIC}_s}$, $\Delta\gamma_{\text{TA}_s}$, $\Delta\gamma_{\text{T}}$, $\Delta\gamma_{\text{S}_{fw}}$, and $\Delta\delta\text{DIC}_s$, $\Delta\delta\text{TA}_s$, $\Delta\delta\text{T}$, $\Delta\delta\text{S}_{fw}$ respectively. Finally, we introduce the vector \mathbf{X} formed by the four variables DIC_s , TA_s , T and S_{fw} , as: $\{X_0, X_1, X_2, X_3\} = \{\text{DIC}_s, \text{TA}_s, \text{T}, \text{S}\}$. With this notation, we can write an expansion of Eq.(3) of the final state of the system by 2080-2100 named \mathbf{X}^f around the initial state $\mathbf{X}^i = \{\text{DIC}_s^i, \text{TA}_s^i, \text{T}^i, \text{S}_{fw}^i\}$ by 2006-2026 as:

$$\begin{aligned}
\Delta\delta p\text{CO}_2 = & \Delta\overline{p\text{CO}_2} \sum_{k=0}^3 \gamma_{X_k}^i \cdot \delta X_k^i \\
& + \overline{p\text{CO}_2}^i \sum_{k=0}^3 \Delta\gamma_{X_k} \cdot \delta X_k^i \\
& + \overline{p\text{CO}_2}^i \sum_{k=0}^3 \gamma_{X_k}^i \cdot \Delta\delta X_k \\
& + \Delta\overline{p\text{CO}_2} \sum_{k=0}^3 \Delta\gamma_{X_k} \cdot \delta X_k^i \quad (2^{nd} \text{ order terms}) \\
& + \Delta\overline{p\text{CO}_2} \sum_{k=0}^3 \gamma_{X_k}^i \cdot \Delta\delta X_k \\
& + \overline{p\text{CO}_2}^i \sum_{k=0}^3 \Delta\gamma_{X_k} \cdot \Delta\delta X_k \quad , \tag{4}
\end{aligned}$$

where the first, second and third terms represent the contributions to $\Delta\delta p\text{CO}_2$ due to changes in the mean $p\text{CO}_2$ ($\Delta\overline{p\text{CO}_2}$), the $p\text{CO}_2$ sensitivities ($\Delta\gamma_{X_k}$) and the seasonal cycles ($\Delta\delta X_k$) respectively; the fourth to sixth rows are the second order terms. This method is similar to the one used by Landschützer et al. (2018).

3 Results and discussion

3.1 $\delta p\text{CO}_2$ amplification

Figure 1, (a) shows the ensemble mean $\delta p\text{CO}_2$ amplitude (calculated as climatological maximum-minus-minimum) for the initial period 2006-2026. The values range from $\approx 98 \mu\text{atm}$ for the high latitudes ($40^\circ\text{S}-70^\circ\text{S}$, $40^\circ\text{N}-60^\circ\text{N}$) to $\approx 60 \mu\text{atm}$ between $40^\circ\text{S}-40^\circ\text{N}$. The ~~range agrees with previous estimates by Takahashi et al. (2002).~~ ensemble mean initial seasonal amplitude range is in good agreement with observational estimates calculated for the reference year 2005 (Takahashi et al., 2014b), and for the 1982-2015 period (Landschützer et al., 2017). The agreement between models and observations is remarkably good in the equatorial regions, but the initial amplitude is slightly overestimated in the mid and high latitudes (see Supplementary Fig. S3). The higher amplitude in models than observations is expected, as the initial period 2006-2026 already experienced an amplification compared to previous years. Moreover, Tjiputra et al. (2014) found that the ocean's $p\text{CO}_2$ historical trend is

25 larger in models than observations when it is estimated in large scale areas of the ocean. However, they found that models' pCO₂ trends agree with observations when the trends are subsampled to the locations where the observations were taken, and therefore they do a good job reproducing well-known time series. Moreover, differences are expected as Pilcher et al. (2015) suggested that CMIP5 models perform well in reproducing the seasonal cycle timing, but still show considerable errors in reproducing the seasonal amplitude of pCO₂ due to differences in the mechanisms represented in each model, especially in
5 subpolar biomes.

By 2080-2100 the annual cycle amplitude attains values of $\approx 197 \mu\text{atm}$ and $\approx 101 \mu\text{atm}$ in the high and mid-low latitudes respectively (Fig. 1,(b)). These seasonal variations correspond to 20% and 18% of annual $\overline{\text{pCO}_2}$ for the initial and final periods respectively. Figure 1, (c), shows that the global ocean δpCO_2 will intensify by a factor of 1.5 to 3 times for the 2080-2100 period relative to the 2006-2026 reference period. Figure 1, (d), shows the difference in amplitude ($\Delta\delta\text{pCO}_2$); this pattern differs from the ratio, because the ratio overestimates the amplification in areas where the initial amplitude is lower than $\approx 10 \mu\text{atm}$. McNeil and Sasse (2016) ~~using a data-based approach, found~~ used observations and a neural-network-clustering algorithm to project that by year 2100, the δpCO_2 amplitude in some regions could be up to ten times larger than it was in year 2000. Our mean amplification factor estimation agrees with the ~~lower end range of (McNeil and Sasse, 2016)~~ mean threefold amplification
15 found for most of the ocean by McNeil and Sasse (2016). However the high values in this previous study can not be reproduced here - mainly because we consider 21 years average ratios instead of single year ratios, which are strongly affected by interannual variability. Using observations, Landschützer et al. (2018) found an increase of $2.2 \mu\text{atm}$ per decade, which ~~agrees with~~ is smaller than our findings of a ~~mean 20 total 42~~ mean 20 total 42 μatm increase by the end of the century ~~, excluding between 40°S-40°N, and a global-mean change of 81~~ μatm on the high latitudes that exhibit larger changes. This difference is again possibly due
20 the higher mean pCO₂ values in models than observations.

The global ocean mean amplification factor of δpCO_2 roughly coincides with a doubling of $\overline{\text{pCO}_2}$ (Fig. 2). ~~Their direct relation~~ The direct relationship between these two is explained in section 3.5. Figure 1 (e-h) shows the zonal mean panels of (a-d); ~~in~~ In general, towards the end of the century the pCO₂ amplifies more in high latitudes, but so does the standard deviation uncertainty among models. ~~The regional~~ This regional pattern agrees with the observation-based findings of Landschützer et al. (2018)
25 which show that high latitudes have already experienced a larger amplification than mid-low latitudes from 1982 to 2015. Furthermore, the same pattern is projected by CMIP5 models for the seasonal amplification of [H⁺] by the end of the century (Kwiatkowski and Orr, 2018). This is expected from the near-linear relation between pCO₂ and [H⁺]. These regional differences in amplification for pCO₂ can be explained in terms of the relative magnitudes and the phases between the DIC, TA, T and S contributions, which are explained in subsequent sections.

30 **3.2 Present and future drivers of δpCO_2**

To understand the driving factors of δpCO_2 and its spatiotemporal differences, we split δpCO_2 into the four different contributions from DIC_s, TA_s, T and S_{fw} for the initial and final periods, following Eq. (1). The results are shown in Fig. 3. ~~Our~~ For most of the ocean, the ensemble mean estimated contributions from DIC_s and T to the present-day δpCO_2 are in good

agreement with the data-based estimates of ~~Takahashi et al. (2002); Fay and McKinley (2017). Figure 3, shows that between~~ Takahashi et al. (2014b) and Landschützer et al. (2017), particularly in the equatorial regions (see Supplementary Fig. S3). However our T and DIC contributions are slightly larger in mid and high latitudes, for the same reasons the $p\text{CO}_2$ seasonal amplitude is overestimated (see Section 3.1). Also, differences arise between our DIC_s contribution and the observation-based so called "non-thermal" contribution, because the non-thermal contribution also includes the total alkalinity and salinity effects.

5 ~~Nonetheless, between 40°S-40°N, our ensemble mean shows that~~ $\delta p\text{CO}_2$ is dominated by changes in temperature that control CO_2 solubility, which decreases in summer enhancing $p\text{CO}_2$, in agreement with observations. The Southern Ocean is controlled by DIC, that responds to changes in upwelling and phytoplankton blooms. Both mechanisms act together to decrease (increase) DIC in summer (winter) (Sarmiento and Gruber, 2006).

~~In the The models show that the $\delta p\text{CO}_2$ in the 40°N to 60°N band of the Pacific and the Atlantic basins variations are~~ controlled by DIC and T respectively is controlled by T, which disagrees with the above mentioned observations that show a non-temperature dominance in this band. The difference between models and observations arises from two regions: the North Atlantic basin and the North Western Pacific; specifically near the Oyashio Current, and the outflows from the Okhotsk Seas (see Supplementary Fig. S3). Most models show a T dominance in the North Atlantic basin; only CESM1-BGC and GFDL-ESM2M show a DIC dominance (see Supplementary ~~information Fig. S2)-Fig. S4).~~ Fig. S4). The North Atlantic is one of the

15 major sinks of anthropogenic CO_2 , however some models fail to estimate its uptake capacity (Goris et al., 2018). Goris et al. (2018) found that models with an efficient carbon sequestration present a DIC-dominated $p\text{CO}_2$ seasonal cycle in the North Atlantic, but models with low anthropogenic uptake show a T dominance in this region. In the North-Western Pacific, Mckinley et al. (2006) found that coarse models are not able to capture the intricate oceanographic features of this area, and therefore the $p\text{CO}_2$ seasonality is not well captured.

20 Towards the end of the century (Fig. 3, right column), the amplification of $\delta p\text{CO}_2$ is caused by an increase in the DIC_s and T contributions, and to a lesser extent due to TA_s and S_{fw} . Only in the high latitudes the TA_s contribution reinforces the DIC_s effect. The δDIC_s and δT relative phase and magnitude play an important role in causing regional differences of future $\delta p\text{CO}_2$. For example, between 40°-60°, we find a lower amplification factor than at 30°-40° in both hemispheres (Fig. 1, (c)), contrary to what we expected from the general observed larger amplification at higher latitudes. In this band of lower amplification, the

25 warm water from subtropical regions meets the nutrient rich water from the subpolar regions, but the DIC_s and T effects are almost 6 months out of phase, and therefore their cancellation is larger than in the 30°-40° latitude band; where for example, in the North Atlantic, there is 9 month phase-difference between both contributions. A clear illustration of this phase effect is found in the Supplementary information (Fig. S5).

In the Southern Ocean there is a shift in the maximum $\delta p\text{CO}_2$ occurring from August-September to March-April (Fig. 3, last

30 row). This shift is generated because the T contribution gains importance over DIC_s , due to a reduction of δDIC_s magnitude ~~and a small increment of at the same time that δT increases~~ (Fig. 5). In the Equatorial Pacific region (Fig. 5), T dominates over DIC_s but both contributions are small due to their low seasonality ~~(Fig. 5)-.~~ Therefore, this region will experience a low amplification in $\delta p\text{CO}_2$. In this region some models underestimate the $p\text{CO}_2$ trend (Tjiputra et al., 2014), and therefore the seasonal amplification might be underestimated too. In the following sections we conduct further analysis by decomposing

each contribution as the result of three factors: the mean $p\text{CO}_2$ ($\overline{p\text{CO}_2}$), the regional $p\text{CO}_2$ sensitivities (γ_{DIC} , γ_{TA} , γ_{T} and $\gamma_{\text{S}_{\text{fw}}}$) and the seasonal cycles ($\delta\text{DIC}_{\text{s}}$, $\delta\text{TA}_{\text{s}}$, δT and $\delta\text{S}_{\text{fw}}$) as determined in Eq. (3).

3.3 Future $p\text{CO}_2$ sensitivities

The γ_{DIC} and γ_{TA} are projected to increase by the end of the ~~Century~~ century due to a lower ocean buffering capacity produced by increasing temperature and larger background concentrations of DIC (Fassbender et al., 2017). This agrees with our results shown in Fig. 4, which shows that all regions will experience an increase in γ_{DIC} and γ_{TA} . Lower buffer factors (higher sensitivities factors) are found in regions where DIC and TA have similar values, and they ~~reach a minimum where will decrease~~ (increase) as the DIC=TA/TA ratio in the oceans increases (Egleston et al., 2010). The alkalinity sensitivity is negative, as $p\text{CO}_2$ decreases with increasing alkalinity, but we show here the negative of γ_{TA} for better comparison. γ_{TA} will increase (with negative values) more than the DIC sensitivity. However seasonal changes in open-ocean TA_{s} are small, and therefore the total contribution of alkalinity in our analysis is negligible compared to the DIC_{s} and T contributions.

~~In $\gamma_{\text{S}_{\text{fw}}}$ decreases everywhere except in the Western Pacific Warm Pool. In this region $\gamma_{\text{S}_{\text{fw}}}$ increases probably due to future changes in precipitation that enhance the fresh-water effect.~~ In Fig. 4, the sensitivities (γ) are expressed as a percentage change of $p\text{CO}_2$ per unit in DIC, TA, T and S respectively. This follows the approach of Takahashi et al. (1993). ~~γ_{DIC} must not be confused with the~~, however in their paper the authors compute the Revelle factor, which is ~~defined~~ related to γ_{DIC} as $R = \text{DIC} \cdot \gamma_{\text{DIC}}$. To illustrate the meaning of the sensitivities, we will focus on the subtropical North Pacific in the 15°N-40°N latitudinal band. In this region γ_{DIC} indicates an average 0.6% change in $p\text{CO}_2$ per unit of DIC in 2006-2026. Therefore, for a $\delta\text{DIC}_{\text{s}}$ seasonal cycle amplitude of $40 \mu\text{mol}/\text{kg}^{-1}$ and $\overline{p\text{CO}_2} \approx 400 \mu\text{atm}$, the total $\delta p\text{CO}_2$ amplitude equals $96 \mu\text{atm}$. Following the same reasoning, by 2080-2100, γ_{DIC} increases to 0.7% and $\delta\text{DIC}_{\text{s}}$ decreases to $30 \mu\text{mol}/\text{kg}^{-1}$; therefore, for a $\overline{p\text{CO}_2}$ equal to $800 \mu\text{atm}$, the $\delta p\text{CO}_2$ ~~annual cycle amplitude change due to~~ amplitude due to δDIC amounts to $168 \mu\text{atm}$. The temperature sensitivity has been experimentally determined by Takahashi et al. (1993); who found a value of 0.0423, meaning that $p\text{CO}_2$ changes by about 4% for every °C. This value agrees with our global mean ensemble estimate of ~~0.0417~~ 0.0428. However, our analytical expression of γ_{T} shows that this value varies regionally and, by reasons unknown to us, it might decrease in the future to a global mean value of ~~0.035~~ 0.0415, (Fig. 4, row (c), third column). The T sensitivity is larger in colder regions and lower in the warmer tropics; however, colder regions will experience a larger reduction on γ_{T} , which locally prevents a larger amplification of the T contribution to $\delta p\text{CO}_2$. In the next section we show that the T seasonality is projected to increase in high latitudes, strengthening the T contribution.

3.4 Future $\delta\text{DIC}_{\text{s}}$, $\delta\text{TA}_{\text{s}}$, δT and $\delta\text{S}_{\text{fw}}$.

Towards the end of the century, the global mean amplitude of $\delta\text{DIC}_{\text{s}}$ is projected to decrease by $\approx 26\text{-}28\%$ in the high latitudes (Fig.5, (a)), according to all the ~~models~~ CMIP5 earth system model simulations used here. In the mid-low latitudinal band there is no agreement between models; while some show an increase others project a decrease in amplitude. As suggested by Landschützer et al. (2018), the larger decrease in the Southern Ocean may be the result of changes in the shallow overturning circulation that prevent CO_2 accumulation in this region. This reduction may be counteracted by the predicted increase in

productivity owing to a suppression of light and temperature limitations (Steinacher et al., 2010; Bopp et al., 2013).

According to the CMIP5 models, most of the ocean is projected to experience a ~~small-slight~~ increase in δT , ~~with lower temperatures in winter and higher in summer~~, as shown in Fig. 5, column (b). All models show a slight increase in δT , only one model showed a slightly decrease in the southern region, and two models showed a decrease in the equatorial region during October to December. ~~The-It is important to note that Fig. 5 shows the seasonal values, with the mean T removed. Therefore,~~
5 ~~when considering the positive T trends, the absolute summer values show an increase and the absolute winter values a decrease. This agrees with the results of Alexander et al. (2018); who showed that models project a seasonal intensification of T, with larger warm extremes and reduced cold extremes. The authors attributed the T seasonality intensification is-consistent-with to an increased oceanic stratification and an overall shoaling of the mixed layer depth, which confines seasonal changes in a reduced volume of water, producing larger changes at the surface. They also showed that the intensification trends are stronger in~~
10 ~~summer than winter, as the mixed layer depth is shallower in summer. Moreover, ice covered regions will experience the largest increase in T seasonality due the loss of sea ice, because the ice melting/freezing moderates the surface water temperature seasonality(Carton et al., 2015).~~

The TA seasonality is also projected to increase in the high latitudes according to all models, except CESM1-BGC ~~that showed-which shows~~ a decrease. For δS (see Supplementary Fig. S6) there is no agreement among ~~the different CMIP5~~
15 ~~models, except in the Southern Ocean where all the models show a slightly decrease. Our-work-demonstrate-that-the-four Kwiatkowski and Orr (2018) demonstrated that the seasonality of the drivers is important to determine future changes in $[H^+]$ seasonality. In the same fashion, our results show that the four δpCO_2 drivers present changes on-in~~ seasonality, and in particular δDIC_s and δT changes are important to explain future projections of the δpCO_2 amplitude. The increase in δT enhances the δpCO_2 amplification, and the reduction of δDIC_s in the Southern Ocean locally prevents a larger amplification.

20 3.5 Regional dominant factors

To identify the main cause of the δpCO_2 amplification we use the Taylor's ~~s-series~~ expansion method. With this method we consider the system's final state (δpCO_2 by 2080-2100) as a perturbation of the initial state (δpCO_2 by 2006-2026), as shown in Eq. (4). The expansion is done in three groups of variables: the seasonal cycles of DIC_s , TA_s , T and S (δX), the sensitivities of pCO_2 to the same four variables (γ_x), and the mean pCO_2 ($\overline{pCO_2}$). Therefore, each term of the expansion represents how
25 much of the total δpCO_2 change (indicated by $\Delta \delta pCO_2$ and calculated as 2080-2100 value- minus-2006-2026 value) is due the change in each of these factors. We also add the second order terms that come from their combination. The results are shown in Fig. 6, (a) and they indicate that the leading cause of the δpCO_2 amplification is the change in $\overline{pCO_2}$ ($\Delta \overline{pCO_2}$),
~~which confirms previous findings by Landschützer et al. (2018).~~

It is important to note that our linear Taylor's expansion approach neglects one aspect of the highly non linear carbonate
30 chemistry of the ocean: it assumes $\overline{pCO_2}$ and the sensitivities as independent variables, and therefore does not include the positive feedback between larger $\overline{pCO_2}$ and increasing γ_{DIC} (decreasing buffering capacity). Hence in the following, we use changes in $\overline{pCO_2}$ and changes in seawater carbonate chemistry synonymously, overall resulting in an enhanced response of δpCO_2 to seasonal changes in DIC, TA, T and S.

Considering regional differences, we note that the amplification increases as we move poleward in spite of decreasing $\Delta\overline{pCO_2}$ (see Fig. 1 and 2). This characteristic geographical pattern of stronger high latitude amplification is the result of larger present-day sensitivities (γ_{DIC_s} , γ_T) and seasonal amplitudes (δDIC_s , δT) in the high latitudes that amplify the effect of $\Delta\overline{pCO_2}$ even when its value is small compared to other regions (see Eq. (4), first row term). Some exceptions can be found south of Greenland and near the subtropical gyres, where $\Delta\overline{pCO_2}$ reaches higher values and therefore they also present large amplification. We also found spatial differences on smaller scales; for example, the western Equatorial Pacific presents lower initial δpCO_2 and amplification than the eastern Equatorial Pacific (see Fig. 1). This is because the eastern side of the basin has larger DIC_s and T contributions than the western side (see Supplementary Fig. S2), as consequence of the upwelling of cold, CO_2 -rich waters in the east, which lower the buffering capacity and induce larger seasonal changes in δpCO_2 amplitude due the seasonal effects of productivity and solubility (Valsala et al., 2014).

To further disentangle which of the two main drivers (DIC_s or T) is most affected by $\Delta\overline{pCO_2}$, we decomposed the DIC_s and T contributions in their sensitivity, seasonal cycle and $\overline{pCO_2}$ components, as shown in Figure 6, (b), shows the total DIC and T components together with the $\Delta\overline{pCO_2}$ and seasonal cycles effects on them. The effects from the sensitivities are not depicted, as they only play a minor role. Only the $\Delta\gamma_{DIC}$ term gains importance in the Southern Ocean (not shown). In most of the ocean, the $\Delta\overline{pCO_2}$ effect on T contribution is the leading cause of amplification. This effect is the result of seasonal solubility changes acting over a larger $[CO_2]$ (Gorgues et al., 2010). In the northern high latitudes, an increase on δT reinforces the amplification. In general, the $\Delta\delta T$ contribution gains importance as we move poleward in both hemispheres and therefore the second order terms originating from $\Delta\overline{pCO_2} \cdot \Delta\delta T$ also reinforce the amplification. Interestingly, in the high latitudes, the amplification through second order terms is as important as the change in the seasonality of the drivers.

The Southern Ocean is an exception to the T dominance; in this region the $\Delta\overline{pCO_2}$ effect on the DIC_s contribution dominates, and the regional amplification is heavily reinforced by low values of the mean buffering capacity (high γ_{DIC_s}), this. This result agrees with the findings of Hauck and Völker (2015). In this southern region area the amplification is only partially counteracted by a reduction in δDIC_s from January to March.

4 Summary and Conclusions

Using In this study, we used output from 7 CMIP5 global models our study provides, subjected to the RCP8.5 radiative forcing scenarios, to provide a comprehensive analysis of the characteristics and drivers of the intensification of the seasonal cycle of pCO_2 between present (2006-2026) and future (2080-2100) conditions. By 2080-2100 the δpCO_2 will be 1.5-3 times larger compared to 2006-2026. We demonstrate that on average The projected amplification by the earth-system models and the possible causes of it, are consistent with observation-based amplification for the period from 1982 to 2015 (Landschützer et al., 2018). However, the models slightly overestimate the present day amplification, probably due the larger pCO_2 trends in models than observations (Tjiputra et al., 2014).

The models confirm the well-established mechanisms controlling present-day δpCO_2 (Takahashi et al., 2002; Sarmiento and Gruber, 2006; DIC_s and T contributions are the main counteracting terms dominating the seasonal evolution of δpCO_2 . Furthermore, the

models show that under future conditions the controlling mechanisms remain unchanged. This result confirms the findings of Landschützer et al. (2018) that identified the same regional controlling mechanism for the past 30 years. The relative role of the DIC and T terms is regionally dependent. High latitudes and upwelling regions, such as the California Current system and the coast of Chile, are dominated by DIC_s and the temperate low latitudes are driven by T. Only in the North Atlantic and North-Western Pacific the models show a dominance of thermal effects over non-thermal effects, which is in disagreement with observations. This further illustrates the urgent need for models to accurately represent regional oceanographic features to accurately reproduce the $\delta p\text{CO}_2$ characteristics.

In agreement with Landschützer et al. (2018), also the model projections towards the end of this century demonstrate that the global amplification of $\delta p\text{CO}_2$ is due to the overall longterm increase of anthropogenic CO₂. A higher oceanic background CO₂ concentration enhances the effect of T-driven solubility changes on $\delta p\text{CO}_2$ and alters the seawater carbonate chemistry, also enhancing the DIC seasonality effect. The spatial differences of $\delta p\text{CO}_2$ amplification, however, are determined by the regional sensitivities γ_{DIC} and seasonality of pCO₂ drivers. For example, polar regions show a larger sensitivity to DIC and T, which lead to and larger seasonal cycles of DIC and T. Therefore, these areas present a strong enhancement of $\delta p\text{CO}_2$, in spite of smaller changes in mean pCO₂.

~~Our results extend and refine the current views, in which the future amplification has been attributed uniquely to the DIC sensitivity (Hauck and Völker, 2015; McNeil and Sasse, 2016; Fassbender et al., 2017). We show that it is crucial to include the changing seasonal cycles of DIC and T. Moreover, the pCO₂ seasonal cycle amplitude depends on the relative magnitude and phase of the contributions. The models ensemble mean reproduces the highly effective compensation of DIC_s and T contributions when they are six months out of phase, confirming previous studies (Takahashi et al., 2002; Landschützer et al., 2018). The compensation of DIC and T prevents a larger amplification of $\delta p\text{CO}_2$, even when both contributions are largely amplified.~~

The amplification of the TA and S contributions have a small impact on $\delta p\text{CO}_2$ in most regions, except in the high latitudes where the TA contribution complements the DIC one, enhancing the non-thermal effect in this region.

The use of earth system models allowed us to state the importance of including future changes on the drivers' seasonalities for future $\delta p\text{CO}_2$ projections. The T seasonality is projected to increase in most of the ocean basins, thereby reinforcing the $\delta p\text{CO}_2$ amplification. The δT increase is consistent with an increase in stratification that will confine the seasonal changes in net heat fluxes to a shallower mixed layer (Alexander et al., 2018). The DIC_{s-s} seasonality decreases in some cold areas and its reduction prevents a larger amplification.

~~The first complete analytical Taylor expansion of $\delta p\text{CO}_2$ in terms of the variables DIC_s, TA_s, T and S showed that DIC_s and T contributions are the main counteracting terms to control the $\delta p\text{CO}_2$, both under present-day and future conditions. The prevalence of one term over the other in various regions remains similar, even under enhanced CO₂ conditions. The relative role of these terms is regionally dependent. High latitudes and upwelling regions, such as the California Current system and the coast of Chile, are dominated by DIC_s and the temperate low latitudes are driven by T. For the sensitivities, while γ_{DIC} increases, γ_T decreases. The later phenomenon needs further study. Moreover, the pCO₂ seasonal cycle amplitude depends on the relative magnitude and phase of the contributions. Spatially,~~

~~we found that the magnitude of the contributions depends on the mean $p\text{CO}_2$, its local sensitivities ($\gamma_{DIC,TA,T,S}$) and the amplitude of their seasonal cycles ($\delta(DIC,TA,T,S)$). The phases depend on the regional characteristics of the seasonal cycles and they moderate the counteracting nature of both contributions. The compensation of DIC_s and T contributions is most effective when they are six months out of phase.~~ The increasing amplitude of $\delta p\text{CO}_2$ might have implications for the net air-sea flux of CO_2 , in particular in regions where there is an imbalance between winter and summer values (Gorgues et al., 2010). Examples of such behavior can be found in the Southern Ocean (between 50°S - 60°S) (Takahashi et al., 2014a) and in the latitude band from 20° - 40° in both hemispheres (Landschützer et al., 2014). Moreover, seasonal events of high $p\text{CO}_2$ could have an impact on acidification and aragonite undersaturation events (Sasse et al., 2015) and hypercapnia conditions (McNeil and Sasse, 2016). Therefore, understanding the drivers of future $\delta p\text{CO}_2$ may help to better assess the response of marine ecosystems to future changes in carbonate chemistry. Finally, our complete analytical expansion of $\delta p\text{CO}_2$ in terms of all its 4 variables provides a practical tool to accurately and quickly diagnose temperature and salinity sensitivities from observational or ~~modeling~~ modelling datasets.

10 5 Acknowledgements

This work was supported by the National Science Foundation under Grant No. 1314209 and by the Institute for Basic Science (IBS), South Korea under IBS-R028-D1. We thank Peter Landschützer for kindly providing his data-sets of thermal and non-thermal components of the $p\text{CO}_2$ seasonal cycle.

References

- 15 Alexander, M. A., Scott, J. D., Friedland, K. D., Mills, K. E., Nye, J., Pershing, A. J., and Thomas, A. C.: Projected sea surface temperatures over the 21st century: Changes in the mean, variability and extremes for large marine ecosystem regions of Northern Oceans, *Elem. Sci. Anth.*, 6, 9, 2018.
- Bopp, L., Resplandy, L., Orr, J. C., Doney, S. C., Dunne, J. P., Gehlen, M., Halloran, P., Heinze, C., Ilyina, T., Safarian, R., Tjiputra, J., and Vichi, M.: Multiple stressors of ocean ecosystems in the 21st century: projections with CMIP5 models, *Biogeosciences*, 10, 6225–6245, 2013.
- 20 Carton, J. A., Ding, Y., and Arrigo, K. R.: The seasonal cycle of the Arctic Ocean under climate change, *Geophys. Res. Lett.*, 42, 7681–7686, 2015.
- Egleston, E. S., Sabine, C. L., and Morel, F. M. M.: Revelle revisited: Buffer factors that quantify the response of ocean chemistry to changes in DIC and alkalinity, *Global Biogeochem. Cycles*, 24, GB1002, 2010.
- 25 Fassbender, A. J., Sabine, C. L., and Palevsky, H. I.: Nonuniform ocean acidification and attenuation of the ocean carbon sink, *Geophys. Res. Lett.*, 44, 8404–8413, 2017.
- Fay, A. R. and McKinley, G. A.: Correlations of surface ocean pCO₂ to satellite chlorophyll on monthly to interannual timescales, *Global Biogeochem. Cycles*, 31, 436–455, 2017.
- Gorgues, T., Aumont, O., and Rodgers, K. B.: A mechanistic account of increasing seasonal variations in the rate of ocean uptake of anthropogenic carbon, *Biogeosciences*, 7, 2581–2589, 2010.
- 30 Goris, N., Tjiputra, J., Olsen, A., Schwinger, J., Lauvset, S. K., and Jeansson, E.: Constraining projection-based estimates of the future North Atlantic carbon uptake, *Journal of Climate*, 31(10), 3959–3978, 2018.
- Hagens, M. and Middelburg, J. J.: Attributing seasonal pH variability in surface ocean waters to governing factors, *Geophys. Res. Lett.*, 43, 12,528–12,537, 2016.
- 35 Hauck, J. and Völker, C.: Rising atmospheric CO₂ leads to large impact of biology on Southern Ocean CO₂ uptake via changes of the Revelle factor, *Geophys. Res. Lett.*, 42, 1459–1464, 2015.
- Hauri, C., Friedrich, T., and Timmermann, A.: Abrupt onset and prolongation of aragonite undersaturation events in the Southern Ocean, *Nat. Clim. Change*, 6, 172–176, 2015.
- IPCC: IPCC Climate Change 2013: The Physical Science Basis. Contribution of Working Group I to the Fifth Assessment Report of the Intergovernmental Panel on Climate Change, 2013.
- 5 Kwiatkowski, L. and Orr, J.: Diverging seasonal extremes for ocean acidification during the twenty-first century, *Nat. Clim. Change*, 8, 141–145, 2018.
- Landschützer, P., Gruber, N., Bakker, D. C. E., and Schuster, U.: Recent variability of the global ocean carbon sink, *Global Biogeochem. Cycles*, 28, 927–949, 2014.
- Landschützer, P., Gruber, N., and Bakker, D.: An updated observation-based global monthly gridded sea surface pCO₂ and air-sea CO₂ flux product from 1982 through 2015 and its monthly climatology (NCEI Accession 0160558). Version 2.2. NOAA National Centers for Environmental Information. Dataset. doi:10.7289/V5Z899N6, 2017.
- 10 Landschützer, P., Gruber, N., Bakker, D. C. E., Stemmler, I., and Six, K. D.: Strengthening seasonal marine CO₂ variations due to increasing atmospheric CO₂, *Nat. Clim. Change*, 8, 146–150, 2018.

- Le Quéré, C. L., Moriarty, R., Andrew, R. M., Canadell, J. G., Sitch, S., Korsbakken, J. I., Friedlingstein, P., Peters, G. P., Andres, R. J.,
15 Boden, T. A., Houghton, R. A., House, J. I., Keeling, R. F., Tans, P., Arneeth, A., Bakker, D. C. E., Barbero, L., Bopp, L., Chang, J.,
Chevallier, F., Chini, L. P., Ciais, P., Fader, M., Feely, R. A., Gkritzalis, T., Harris, I., Hauck, J., Ilyina, T., Jain, A. K., Kato, E., Kitidis, V.,
Goldewijk, K. K., Koven, C., Landschützer, P., Lauvset, S. K., Lefevre, N., Lenton, A., Lima, I. D., Metzl, N., Millero, F., Munro, D. R.,
Murata, A., Nabel, J. E., Nakaoka, S., Nojiri, Y., O'Brien, K., Olsen, A., Ono, T., Perez, F. F., Pfeil, B., Pierrot, D., Poulter, B., Rehder,
20 G., Rödenbeck, C., Saito, S., Schuster, U., Schwinger, J., Séférian, R., Steinhoff, T., Stocker, B. D., Sutton, A. J., Takahashi, T., Tilbrook,
B., I. T. van der Laan-Luijkx, I. T., van der Werf, G. R., van Heuven, S., Vandemark, D., Viovy, N., Wiltshire, A., Zaehle, S., and Zeng,
N.: Global Carbon Budget 2015, *Earth Syst. Sci. Data*, 7, 349–396, 2015.
- Lovenduski, N. S., Gruber, N., Doney, S. C., and Lima, I. D.: Enhanced CO₂ outgassing in the Southern Ocean from a positive phase of the
Southern Annular Mode, *Global Biogeochem. Cycles*, 21, GB2026, 2007.
- Mckinley, G. A., Takahashi, T., Buitenhuis, E., Chai, F., Christian, J. R., Doney, S. C., Jiang, M., Lindsay, K., Moore, J. K., Quere, C. L., Lima,
25 I., Murtugudde, R., Shi, L., and Wetzel, P.: North Pacific carbon cycle response to climate variability on seasonal to decadal timescales, *J.*
Geophys. Res., 111, C07S06, 2006.
- McNeil, B. I. and Sasse, T. P.: Future ocean hypercapnia driven by anthropogenic amplification of the natural CO₂ cycle, *Nature*, 529,
383–386, 2016.
- Pilcher, D. J., Brody, S. R., Johnson, L., and Bronselaer, B.: Assessing the abilities of CMIP5 models to represent the seasonal cycle of
30 surface ocean pCO₂, *J. Geophys. Res. Oceans*, 120, 4625–4637, 2015.
- Sabine, C. L., Feely, R. A., Gruber, N., Key, R. M., Lee, K., Bullister, J. L., Wanninkhof, R., Wong, C., Wallace, D. W. R., Tilbrook, B.,
Millero, F. J., Peng, T. H., Kozyr, A., Ono, T., and Rios, A. F.: The oceanic sink for anthropogenic CO₂, *Science*, 305, 367–371, 2004.
- Sarmiento, J. L. and Gruber, N.: *Ocean Biogeochemical Dynamics*, Princeton University Press, Princeton, New Jersey, USA, 2006.
- Sasse, T., McNeil, B. I., Matear, R., and Lenton, A.: Quantifying the influence of CO₂ seasonality on future aragonite undersaturation onset,
35 *Biogeosciences*, 12, 6017–6031, 2015.
- Shaw, E. C., McNeil, B. I., Tilbrook, B., Matear, R., and Bates, M. L.: Anthropogenic changes to seawater buffer capacity combined with
natural reef metabolism induce extreme future coral reef CO₂ conditions, *Glob. Change Biol.*, 19, 1632–1641, 2013.
- Steinacher, M., Joos, F., Froelicher, T. L., Bopp, L., Cadule, P., Cocco, V., Doney, S. C., Gehlen, M., Lindsay, K., Moore, J. K., Schneider,
B., and Segschneider, J.: Projected 21st century decrease in marine productivity: a multi-model analysis, *Biogeosciences*, 7, 979–1005,
2010.
- Takahashi, T., Olafsson, J., Goddard, J. G., Chipman, D. W., and Sutherland, S. C.: Seasonal variation of CO₂ and nutrients in the high-
latitude surface oceans: A comparative study, *Global Biogeochem. Cycles*, 7, 843–878, 1993.
- 5 Takahashi, T., Sutherland, S. C., Sweeney, C., Poisson, A., Metzl, N., Tilbrook, B., Bates, N., Wanninkhof, R., Feely, R. A., Sabine, C. L.,
Olafsson, J., and Nojiri, Y.: Global sea-air CO₂ flux based on climatological surface ocean pCO₂, and seasonal biological and temperature
effects, *Deep-Sea Research II*, 49, 1601–1623, 2002.
- Takahashi, T., Sutherland, S. C., Chipman, D. W., Goddard, J. G., Cheng, H., Newberger, T., Sweeney, C., and Munro, D. R.: Climatological
distributions of pH, pCO₂, total CO₂, alkalinity, and CaCO₃ saturation in the global surface ocean, and temporal changes at selected
locations, *Mar. Chem.*, 164, 95–125, 2014a.
- Takahashi, T., Sutherland, S. C., Chipman, D. W., Goddard, J. G., Newberger, T., and Sweeney, C.: Climatological Distributions of pH, pCO₂,
Total CO₂, Alkalinity, and CaCO₃ Saturation in the Global Surface Ocean. ORNL/CDIAC-160, NDP-094. Carbon Dioxide Information
435 Analysis Center, <https://doi.org/10.3334/CDIAC/OTG.NDP094>, 2014b.

- Tjiputra, J. F., Olsen, A. R. E., Bopp, L., Lenton, A., Pfeil, B., Roy, T., Segsneider, J., Totterdell, I. A. N., and Heinze, C.: Long-term surface pCO₂ trends from observations and models, *Tellus B*, 66, 23 083, 2014.
- Valsala, V. K., Roxy, M. K., Ashok, K., and Murtugudde, R.: Spatiotemporal characteristics of seasonal to multidecadal variability of pCO₂ and air-sea CO₂ fluxes in the equatorial Pacific Ocean, *J. Geophys. Res. Oceans*, 119, 8987–9012, 2014.
- 440 Völker, C., Wallace, D. W. R., and Wolf-Gladrow, D. A.: On the role of heat fluxes in the uptake of anthropogenic carbon in the North Atlantic, *Global Biogeochem. Cycles*, 16(4), 1138, 2002.
- Zeebe, R. E. and Wolf-Gladrow, D.: *CO₂ in Seawater: Equilibrium, Kinetics, Isotopes*, Elsevier Science, Amsterdam, Netherlands, and Philadelphia, PA, USA, 2001.

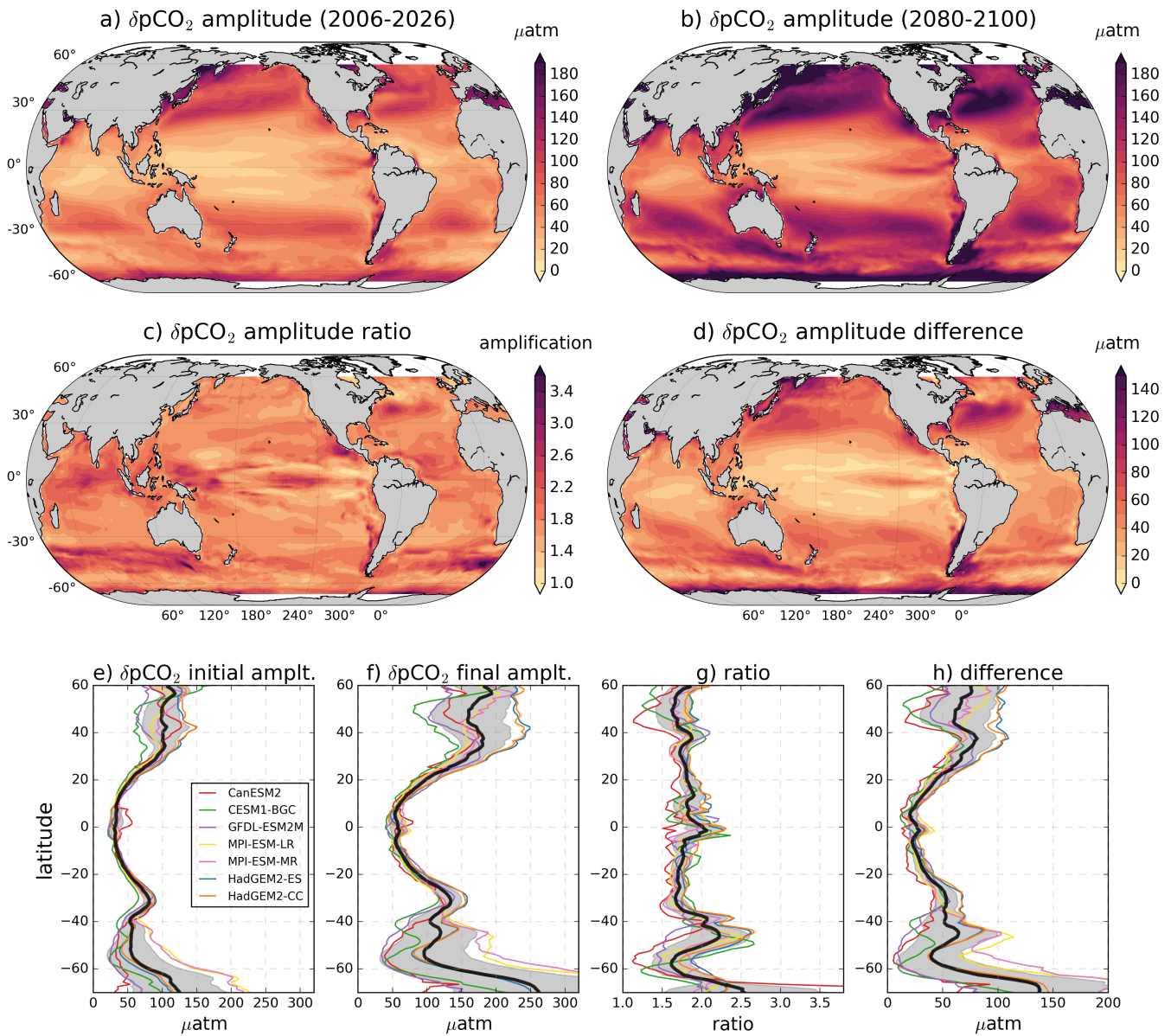


Figure 1. RCP8.5 ensemble mean $p\text{CO}_2$ seasonal cycle amplitude. Amplitude is calculated as climatology maximum-minus-minimum; for a) initial (2006-2026) and b) final (2080-2100) periods. Initial and final climatologies were calculated as the monthly deviation from the respective 21 years period mean. c) and d) show the ratio and difference between the $\delta p\text{CO}_2$ amplitudes for 2080-2100 and 2006-2026 respectively. e) - h) show the zonal mean of a) - d) respectively, with the individual models shown as colored lines and the ensemble mean overlaid in black. Gray shading represents one standard deviation across the models.

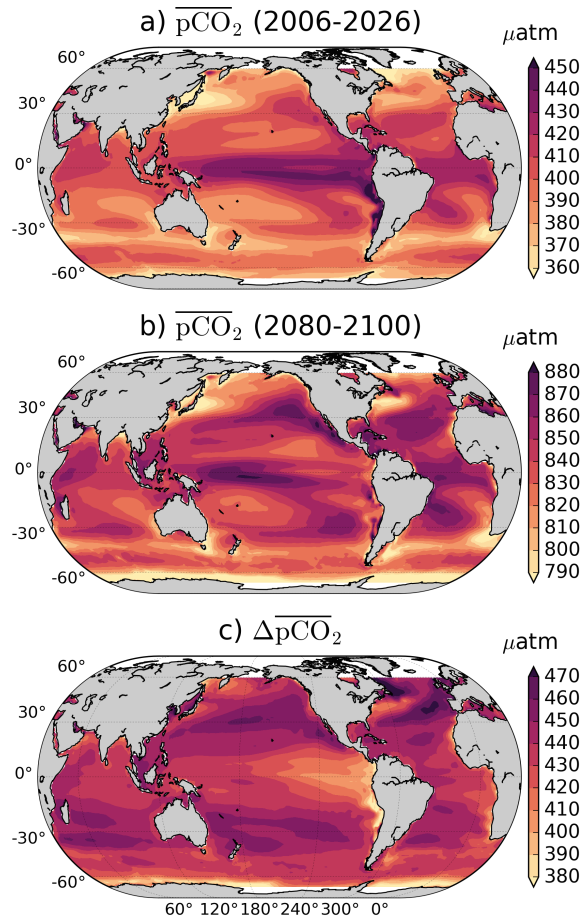


Figure 2. RCP8.5 ensemble mean $\overline{pCO_2}$: by a) 2006-2026 and b) 2080-2100. c) Difference between 2080-2100 and 2006-2026. The North Atlantic and subpolar gyres, show the largest difference between initial and final periods. The scale is different in each plot to enhance regional features.

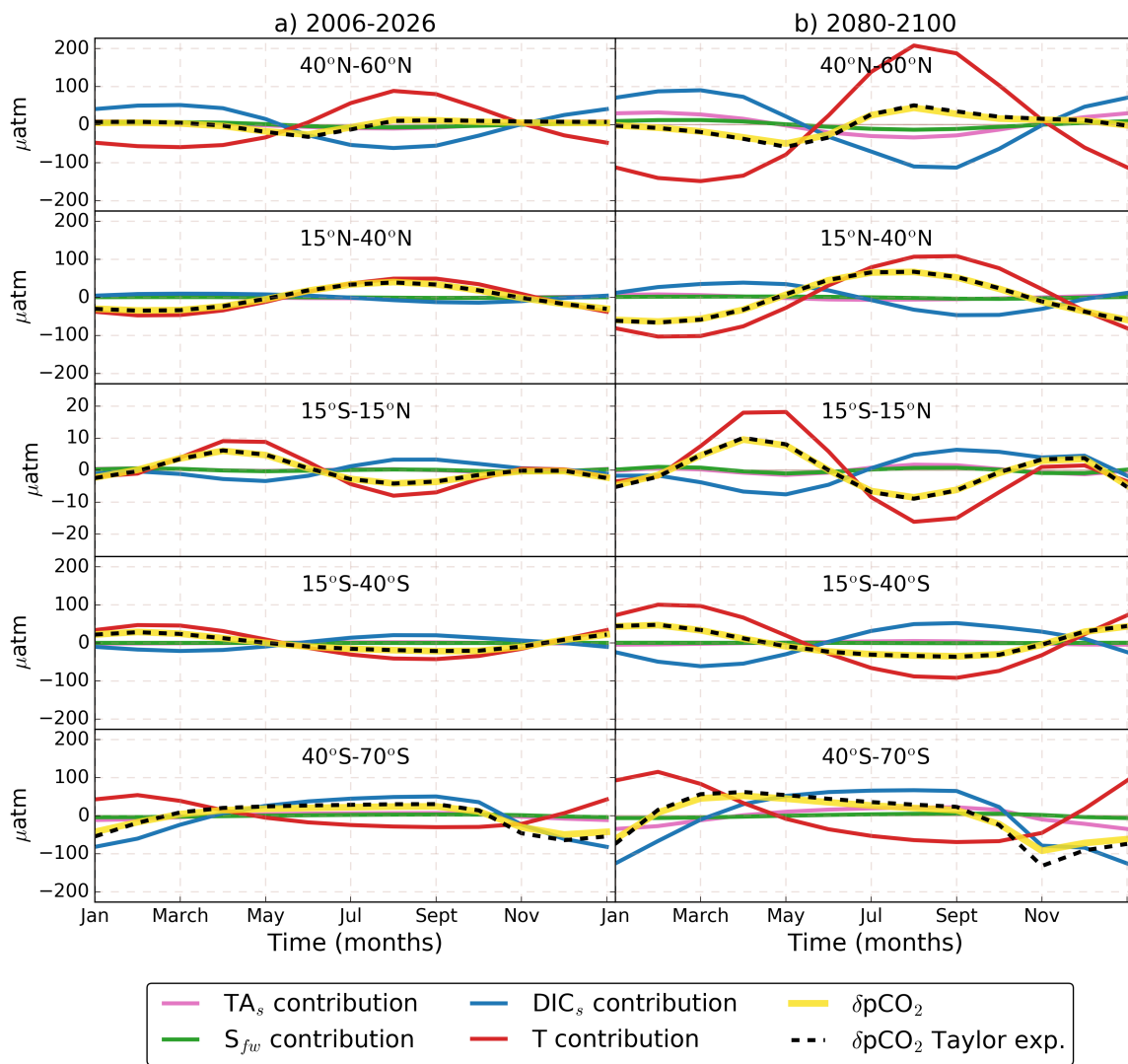


Figure 3. RCP8.5 ensemble mean seasonal cycle ($\delta p\text{CO}_2$) and its Taylor decomposition. Colored lines indicate the contributions of DIC_s (blue), TA_s (pink), T (red) and S_{fw} (green) to $\delta p\text{CO}_2$ reconstructed from its Taylor decomposition (Eq. 1) (dashed black). $\delta p\text{CO}_2$ calculated from monthly $p\text{CO}_2$ (solid yellow) is shown for comparison with the Taylor expansion. Column (a) shows the period 2006-2026 and column (b) shows the period 2080-2100. Each row represents the global zonal average for a different latitudinal band. Temperature dominates all latitudes except the Southern Ocean. In the $40^\circ\text{-}60^\circ\text{N}$ band, T contribution is largely compensated by DIC_s . The TA_s and S_{fw} effects are rather small in all latitudes.

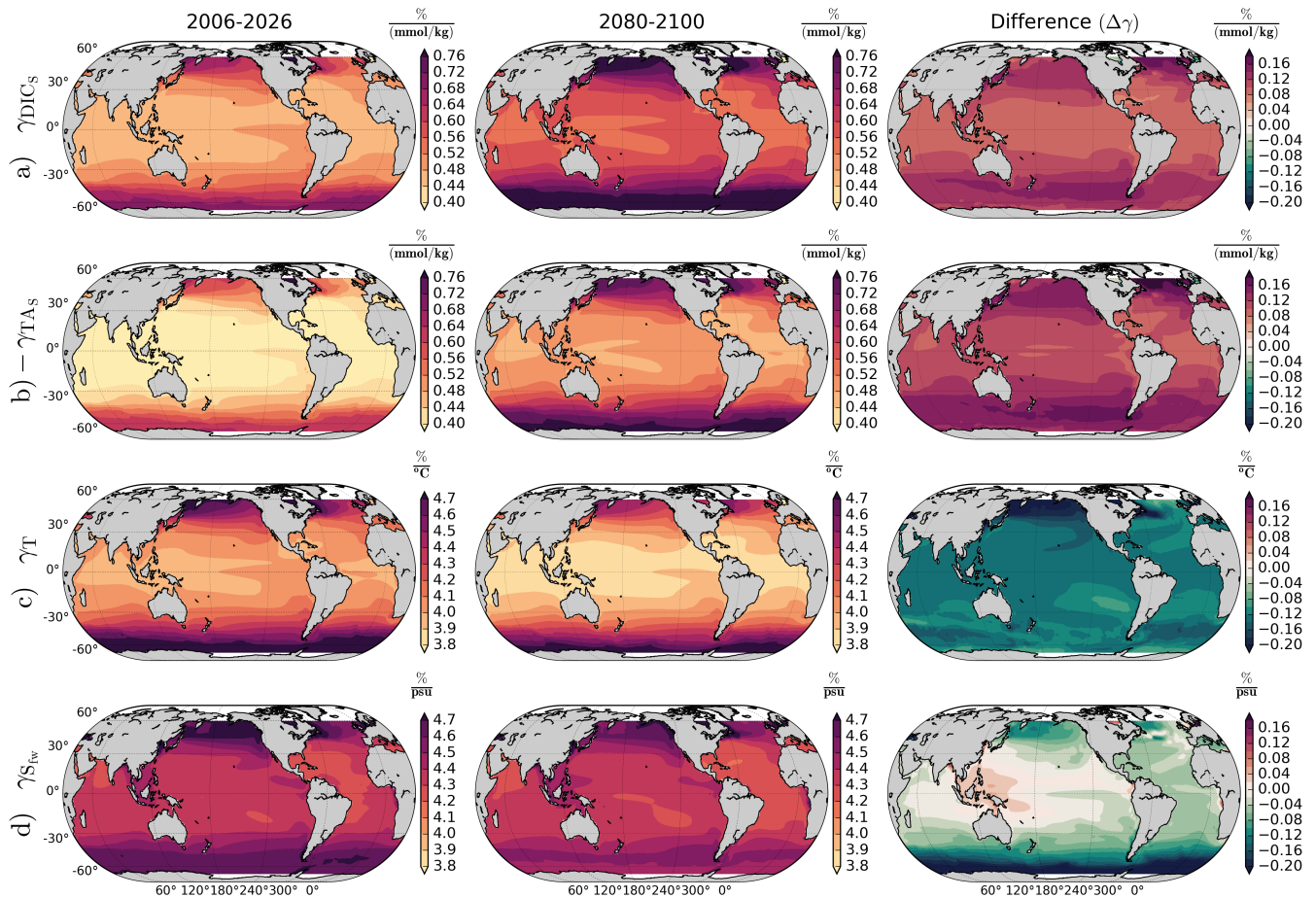


Figure 4. RCP8.5 ensemble mean $p\text{CO}_2$ sensitivities: for DIC_s (row a), TA_s (row b), T (row c) and S_{fw} (row d). Row b) shows the negative of γ_{TA_s} . The first and second columns show the sensitivities by 2006-2026 and 2080-2100 respectively. The third column shows the difference between 2080-2100 and 2006-2026 sensitivities. High latitudes show the largest difference between initial and final periods. While DIC_s and TA_s sensitivities increase, the T and S_{fw} sensitivities decreases, except in the Western Pacific Warm Pool, where $\gamma_{S_{fw}}$ increases.

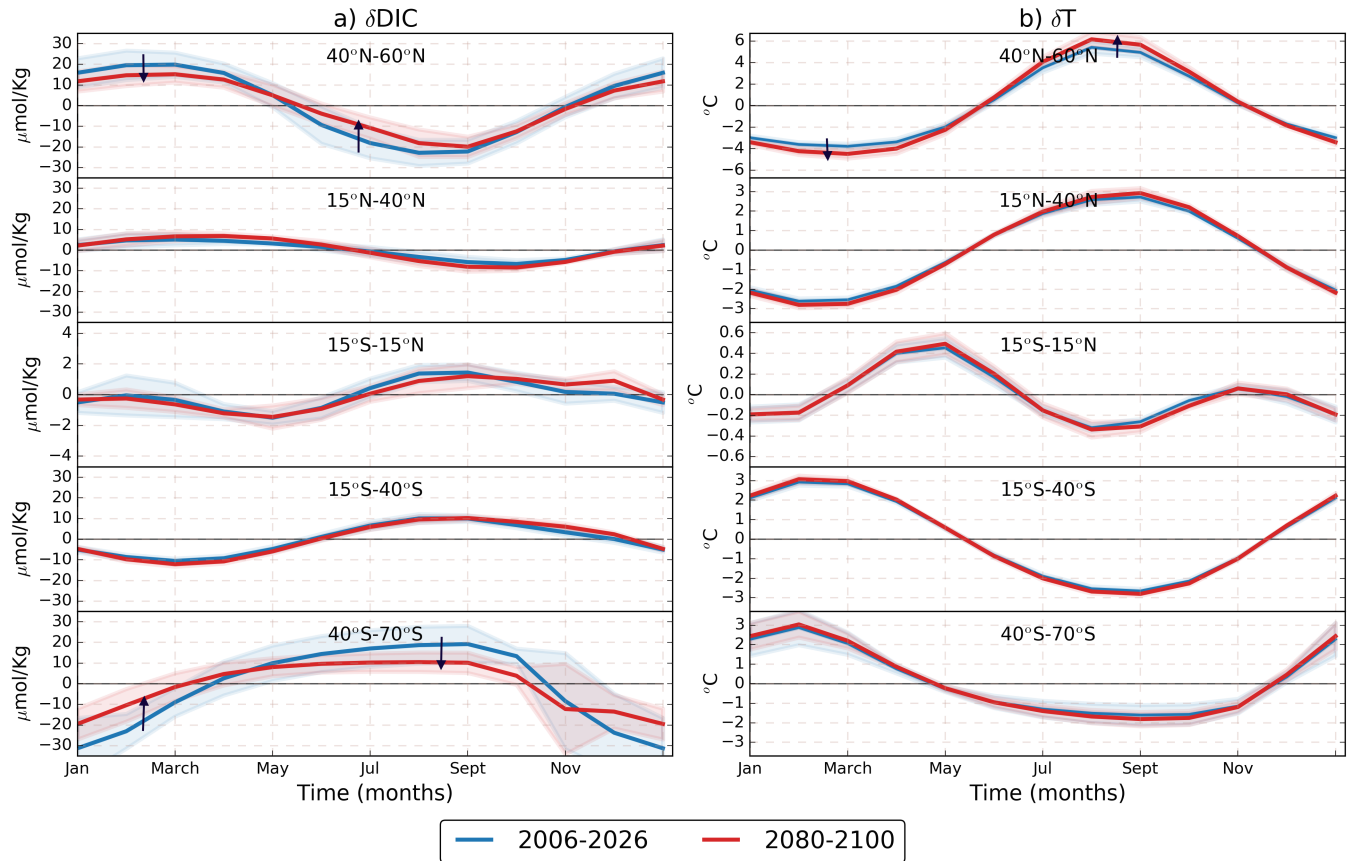


Figure 5. RCP8.5 ensemble zonal mean seasonal cycles: a) δDIC_s and b) δT , for different latitudinal bands. Blue lines represent the 2006-2026 period, depicted for comparison with the 2080-2100 period shown by red lines. Different panels represent different latitudinal sections. Black arrows point out that while T seasonal cycle is projected to increase in most of the ocean, global DIC_s is projected to decrease. The shading represents one standard deviation across the models. It is important to note that the scale is different for some of the latitudinal bands.

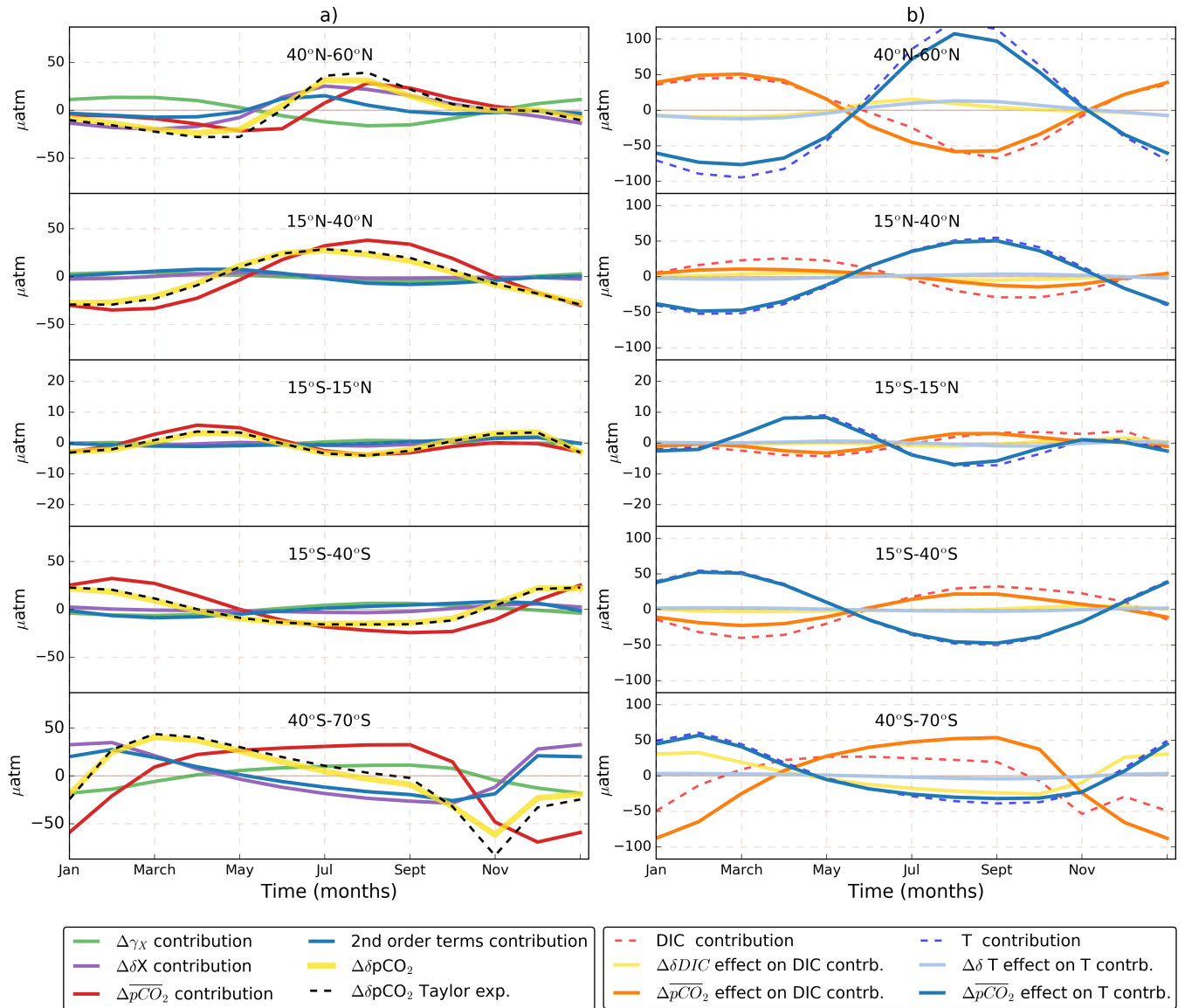


Figure 6. Contribution of seasonalities, sensitivities, and mean $p\text{CO}_2$ changes to $\Delta\delta p\text{CO}_2$. a) Time series for the terms of Eq.(4) for different latitudinal bands. The Δ symbol represents the total century change, calculated as 2080-2100 value -minus- 2006-2026 value. The total change in seasonal $p\text{CO}_2$ ($\Delta\delta p\text{CO}_2$) is depicted as dashed black. This change is decomposed into changes in seasonalities ($\Delta\delta X$, purple), sensitivities ($\Delta\gamma_X$, green), mean $p\text{CO}_2$ ($\Delta\overline{p\text{CO}_2}$, red) and second order terms (blue) summed over the four variables that control $p\text{CO}_2$ (DIC, TA, T and S). For comparison with the expansion, $\Delta\delta p\text{CO}_2$ is calculated from model output (yellow). Column b) shows the total change of DIC (dashed red) and T (dashed blue) contributions. Also shown, are two components of the total change on these contributions; the $\Delta\overline{p\text{CO}_2}$ effect on the DIC (solid orange) and T (solid blue) contributions, and the $\Delta\delta\text{DIC}$ (yellow) and $\Delta\delta\text{T}$ (light blue) effects. In column a), the $\delta p\text{CO}_2$ change follows the $\Delta\overline{p\text{CO}_2}$ effect. In column b) we see shows that actually, the leading cause of amplification is the $\Delta\overline{p\text{CO}_2}$ effect on the T contribution. It is important note the different scale between column a) and b). Also, the scale was reduced in the $15^\circ\text{S}-15^\circ\text{N}$ region to highlight its features.

Text S1.

We construct the full pCO₂ Taylor expansion decomposition starting with the carbonate chemistry definitions of DIC and TA as in Egleston et al. (2010):

$$DIC = [CO_2] + \frac{K_1[CO_2]}{[H^+]} + \frac{K_1K_2[CO_2]}{[H^+]^2} \quad (1)$$

$$TA = \frac{K_1[CO_2]}{[H^+]} + 2\frac{K_1K_2[CO_2]}{[H^+]^2} + \frac{B_{tot}K_b}{(K_b + [H^+])} - [H^+] + \frac{K_w}{[H^+]} \quad (2)$$

Where K_1 and K_2 are defined as Millero et al. (2006), K_w as Millero (1995) and K_b according to Dickson (1990). From Eq.(1) we can obtain $[H^+]$ and from Eq.(2) we get $[CO_2]$ respectively as:

$$[H^+] = \frac{K_1[CO_2] + \sqrt{K_1^2[CO_2]^2 + 4K_1K_2[CO_2](DIC - [CO_2])}}{2(DIC - [CO_2])} \quad (3)$$

$$[CO_2] = \frac{[H^+]^2}{K_1[H^+] + 2K_1K_2} \left(TA - \frac{B_{tot}K_b}{(K_b + [H^+])} + [H^+] - \frac{K_w}{[H^+]} \right) \quad (4)$$

For $[H^+]$ the positive solution was chosen; the negative root gives a result far from real values. From Eq.(3) and Eq.(4) we can make a Taylor's expansion of $[H^+]$ and $[CO_2]$ respectively as:

$$\delta[H^+] = \frac{\partial[H^+]}{\partial DIC} \Big|_{\frac{CO_2, DIC}{T, S}} \delta DIC + \frac{\partial[H^+]}{\partial [CO_2]} \Big|_{\frac{CO_2, DIC}{T, S}} \delta [CO_2] + \frac{\partial[H^+]}{\partial T} \Big|_{\frac{CO_2, DIC}{T, S}} \delta T + \frac{\partial[H^+]}{\partial S} \Big|_{\frac{CO_2, DIC}{T, S}} \delta S \quad (5)$$

$$\delta[CO_2] = \frac{\partial[CO_2]}{\partial TA} \Big|_{\frac{TA, H}{T, S}} \delta TA + \frac{\partial[CO_2]}{\partial [H^+]} \Big|_{\frac{TA, H}{T, S}} \delta [H^+] + \frac{\partial[CO_2]}{\partial T} \Big|_{\frac{TA, H}{T, S}} \delta T + \frac{\partial[CO_2]}{\partial S} \Big|_{\frac{TA, H}{T, S}} \delta S \quad (6)$$

The overbars indicate the mean values of the variables in which the derivatives are evaluated. Finally, we insert $\delta[H^+]$ from Eq.(5) into Eq.(6), to get $[CO_2]$ in terms of DIC, TA, T and S:

$$\begin{aligned} \delta[CO_2] = & \left[1 - \frac{\partial[CO_2]}{\partial [H^+]} \Big|_{\frac{TA, H}{T, S}} \frac{\partial[H^+]}{\partial [CO_2]} \Big|_{\frac{CO_2, DIC}{T, S}} \right]^{-1} \cdot \left[\frac{\partial[CO_2]}{\partial TA} \Big|_{\frac{TA, H}{T, S}} \delta TA \right. \\ & + \frac{\partial[CO_2]}{\partial [H^+]} \Big|_{\frac{TA, H}{T, S}} \frac{\partial[H^+]}{\partial DIC} \Big|_{\frac{CO_2, DIC}{T, S}} \delta DIC \\ & + \left(\frac{\partial[CO_2]}{\partial T} \Big|_{\frac{TA, H}{T, S}} + \frac{\partial[CO_2]}{\partial [H^+]} \Big|_{\frac{TA, H}{T, S}} \frac{\partial[H^+]}{\partial T} \Big|_{\frac{CO_2, DIC}{T, S}} \right) \delta T \\ & \left. + \left(\frac{\partial[CO_2]}{\partial S} \Big|_{\frac{TA, H}{T, S}} + \frac{\partial[CO_2]}{\partial [H^+]} \Big|_{\frac{TA, H}{T, S}} \frac{\partial[H^+]}{\partial S} \Big|_{\frac{CO_2, DIC}{T, S}} \right) \delta S \right] \quad (7) \end{aligned}$$

Comparing the terms from Eq.(7) to the desired Taylor's expansion:

$$\delta pCO_2 \approx \frac{\partial pCO_2}{\partial DIC} \Big|_{\frac{TA, DIC}{T, S}} \delta DIC + \frac{\partial pCO_2}{\partial TA} \Big|_{\frac{TA, DIC}{T, S}} \delta TA + \frac{\partial pCO_2}{\partial T} \Big|_{\frac{TA, DIC}{T, S}} \delta T + \frac{\partial pCO_2}{\partial S} \Big|_{\frac{TA, DIC}{T, S}} \delta S \quad (8)$$

We can identify the derivatives from Eq.(8), as follows:

$$\begin{aligned}
\left. \frac{\partial pCO_2}{\partial TA} \right|_{\overline{T}, \overline{DIC}}^{\overline{TA}, \overline{DIC}} &= \overline{pCO_2} \cdot \frac{-\overline{TA}_c}{\overline{DIC} \cdot \Theta - \overline{TA}_c^2} & (9) \\
\left. \frac{\partial pCO_2}{\partial DIC} \right|_{\overline{T}, \overline{S}}^{\overline{TA}, \overline{DIC}} &= \overline{pCO_2} \cdot \frac{\Theta}{\overline{DIC} \cdot \Theta - \overline{TA}_c^2} \\
\left. \frac{\partial pCO_2}{\partial T} \right|_{\overline{T}, \overline{S}}^{\overline{TA}, \overline{DIC}} &= \overline{pCO_2} \cdot \frac{1}{\overline{DIC} \cdot \Theta - \overline{TA}_c^2} \left[\overline{TA}_c \cdot \left(\frac{\partial Alk_c}{\partial T} + \frac{\partial [B(OH)_4^-]}{\partial T} + \frac{\partial [OH^-]}{\partial T} \right) - \Theta \cdot \frac{\partial (DIC - [CO_2])}{\partial T} \right] - \frac{\overline{pCO_2}}{\overline{K_0}(T, S)} \frac{\partial K_0(T, S)}{\partial T} \\
5 \quad \left. \frac{\partial pCO_2}{\partial S} \right|_{\overline{T}, \overline{S}}^{\overline{TA}, \overline{DIC}} &= \overline{pCO_2} \cdot \frac{1}{\overline{DIC} \cdot \Theta - \overline{TA}_c^2} \left[\overline{TA}_c \cdot \left(\frac{\partial \overline{TA}_c}{\partial S} + \frac{\partial [B(OH)_4^-]}{\partial S} + \frac{\partial [OH^-]}{\partial S} \right) - \Theta \cdot \frac{\partial (DIC - [CO_2])}{\partial S} \right] - \frac{\overline{pCO_2}}{\overline{K_0}(T, S)} \frac{\partial K_0(T, S)}{\partial S}
\end{aligned}$$

where $\Theta = [HCO_3^-] + 4[CO_3^{2-}] + \frac{[B(OH)_4^-][H^+]}{(k_b + [H^+])} + [H^+] + [OH^-]$ and $\overline{Alk}_c = [HCO_3^-] + 2[CO_3^{2-}]$. Below are some details of the specific concentrations derivatives.

$$\begin{aligned}
\frac{\partial Alk_c}{\partial T, S} &= \frac{[CO_2]}{[H^+]^2} \left(\frac{\partial k_1}{\partial T, S} [H^+] + 2k_1 \frac{\partial k_2}{\partial T, S} + 2k_2 \frac{\partial k_1}{\partial T, S} \right) & (10) \\
10 \quad \frac{\partial (DIC - [CO_2])}{\partial T, S} &= \frac{[CO_2]}{[H^+]^2} \left(\frac{\partial k_1}{\partial T, S} [H^+] + k_1 \frac{\partial k_2}{\partial T, S} + k_2 \frac{\partial k_1}{\partial T, S} \right) \\
\frac{\partial [B(OH)_4^-]}{\partial T} &= \frac{B_{tot}[H^+]}{(k_b + [H^+])^2} \frac{\partial k_b}{\partial T} \\
\frac{\partial [B(OH)_4^-]}{\partial S} &= \frac{B_{tot}[H^+]}{(k_b + [H^+])^2} \frac{\partial k_b}{\partial S} + \frac{k_b}{(k_b + [H^+])} \frac{\partial B_{tot}}{\partial S} \\
\frac{\partial [OH^-]}{\partial T, S} &= \frac{1}{[H^+]} \frac{\partial k_w}{\partial T, S}
\end{aligned}$$

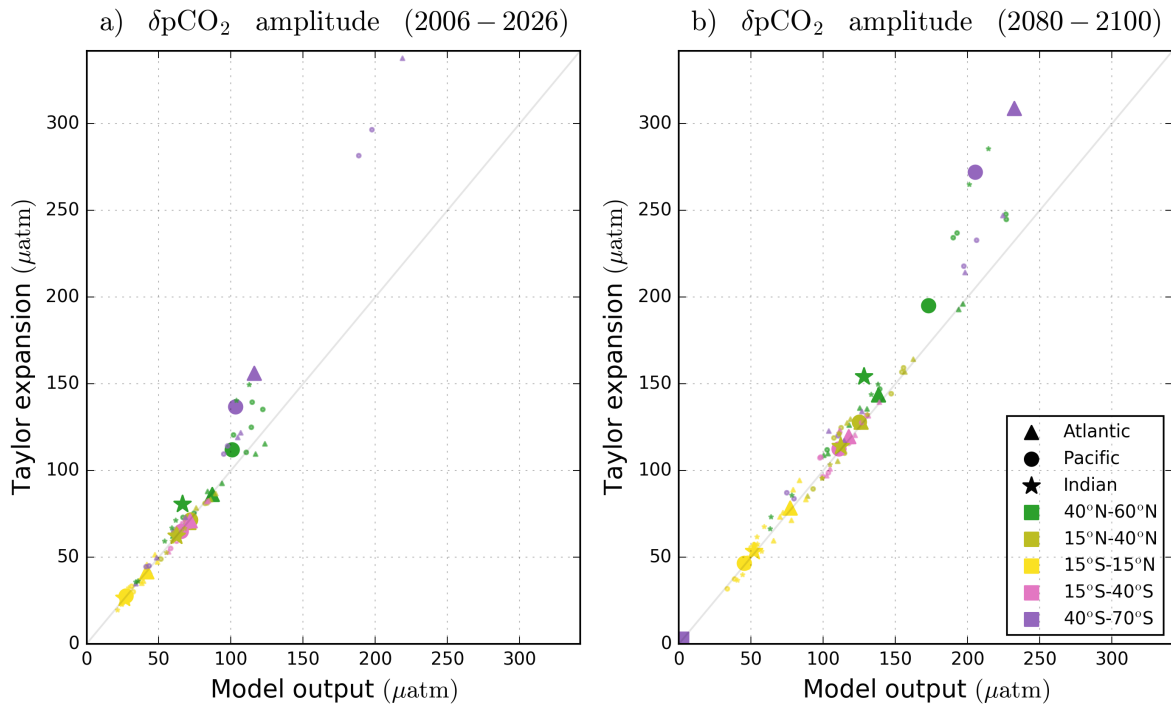


Figure S1. $p\text{CO}_2$ seasonal cycle amplitude calculated from model output compared to its Taylor's expansion reconstruction in a) 2006-2026 and b) 2080-2100. Different colors indicate latitudinal ranges of zonal means, for the Atlantic (triangles), Pacific (circles) and Indian (stars) ocean basins. Large symbols represent the ensemble mean, and small symbols are the result for each model separately.

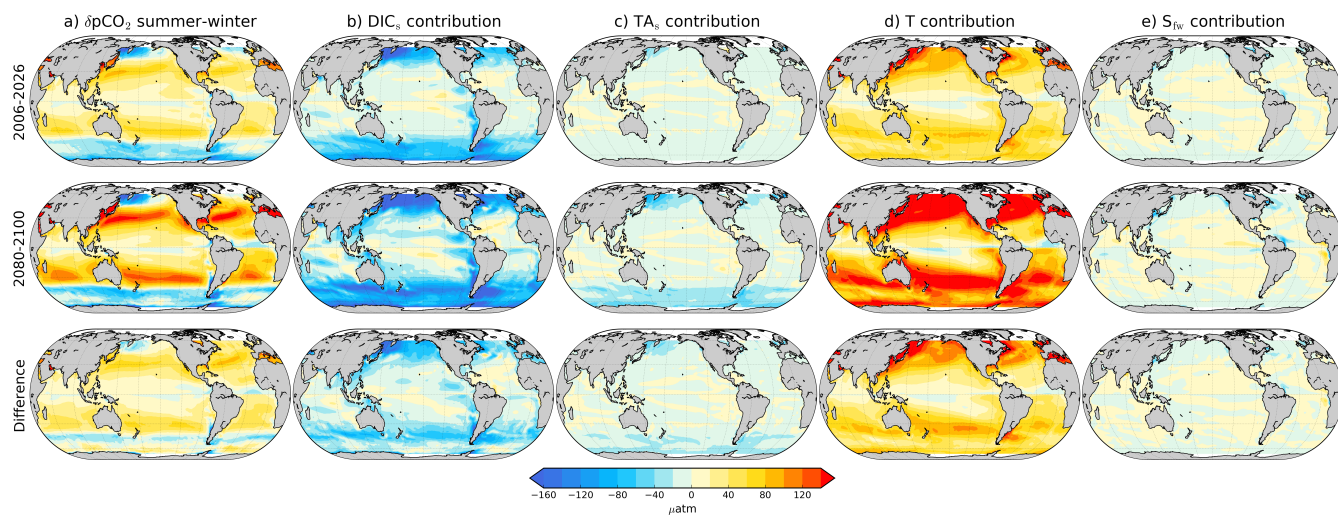


Figure S2. Column a) shows the simulated, ensemble-mean $p\text{CO}_2$ seasonal amplitude calculated as summer minus winter for each hemisphere respectively. b) to e) show DIC_s , T, TA_s and S contributions to the $p\text{CO}_2$ summer-minus-winter amplitude. First and second rows represent respectively the 2006-2026 and 2080-2100 periods. Third row shows the difference between second and first rows. The amplitude was calculated from the climatology for periods 2006-2026 and 2080-2100.

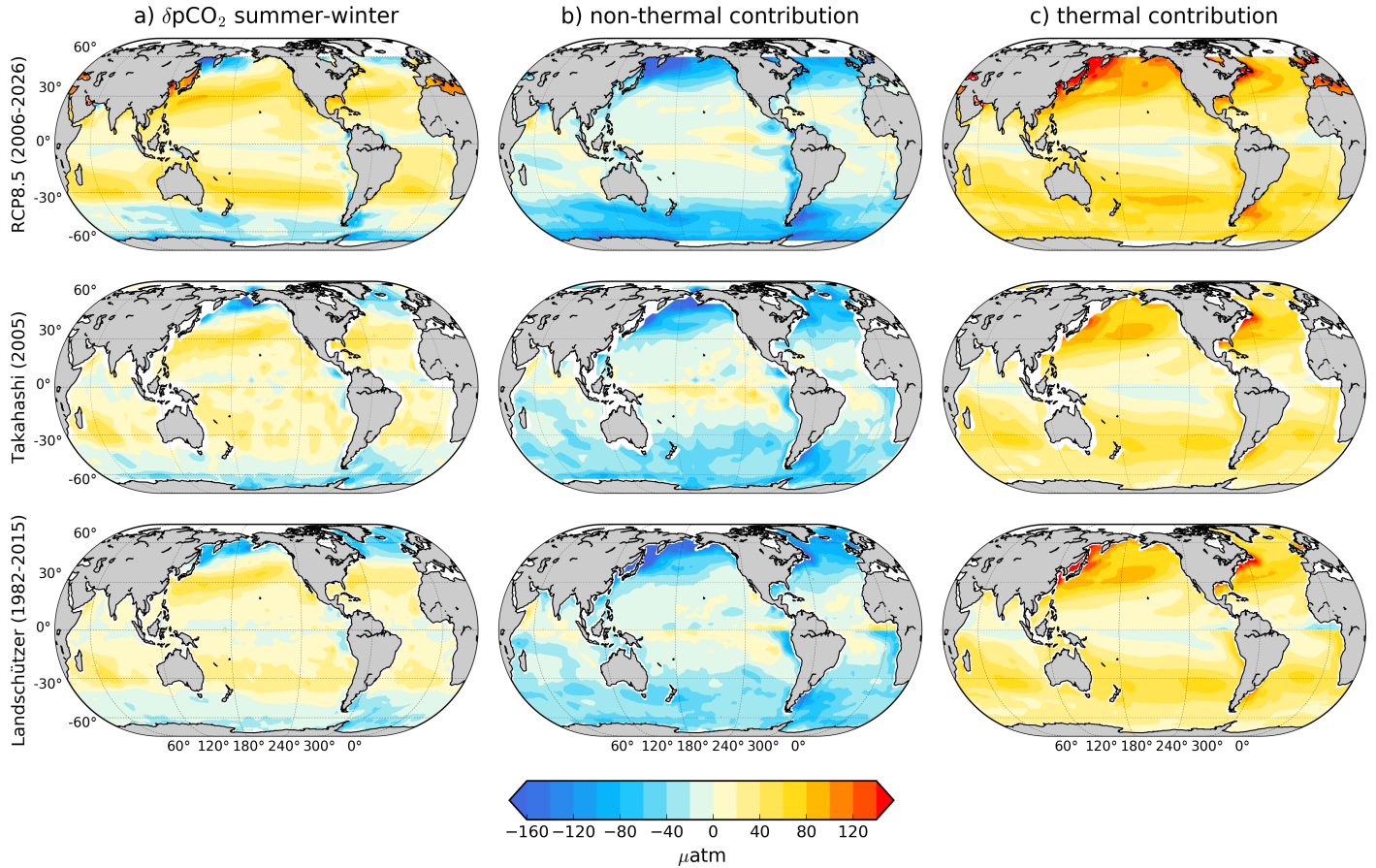


Figure S3. Column a) shows the pCO_2 seasonal amplitude calculated as summer minus winter for each hemisphere respectively. b) and c) show the thermal and non-thermal contributions to pCO_2 seasonality respectively. First row shows CMIP5 models ensemble mean for the 2006-2026 period under the RCP8.5 scenario. Second row shows the estimates from Takahashi et al. (2014) dataset for a reference year 2005, with summer-minus-winter thermal and non-thermal contributions calculated as Takahashi et al. (2002). Third rows show the same components for the Landschützer et al. (2017) pCO_2 data-set, and the thermal and non-thermal estimations that Peter Landschützer facilitated us, for the period 1982-2015.

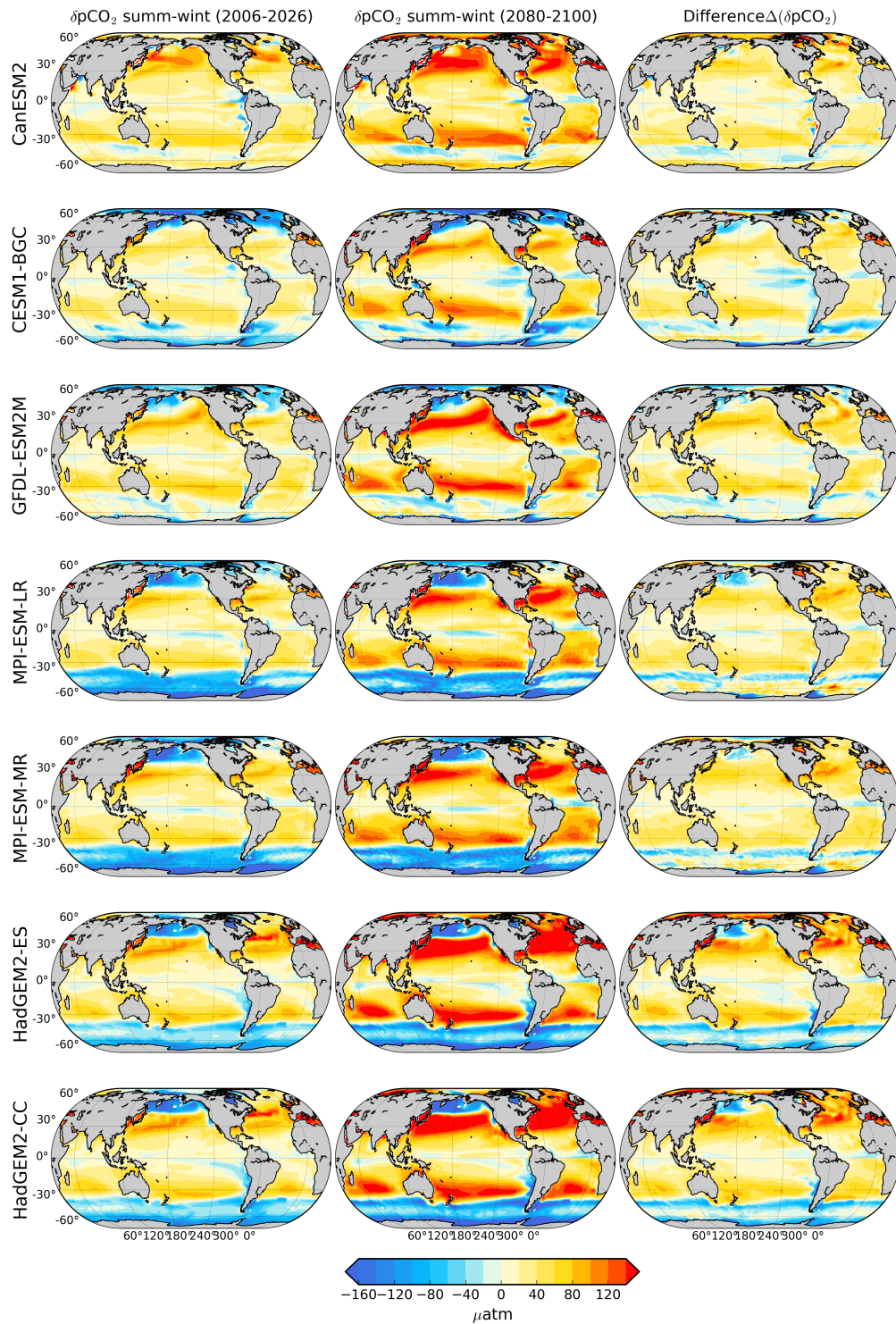


Figure S4. $\delta p\text{CO}_2$ climatology for column a) 2006-2026 and b) 2080-2100 periods calculated as in Fig. S2; each row is the result for a different model. Column c) shows the differences between column b) and a).

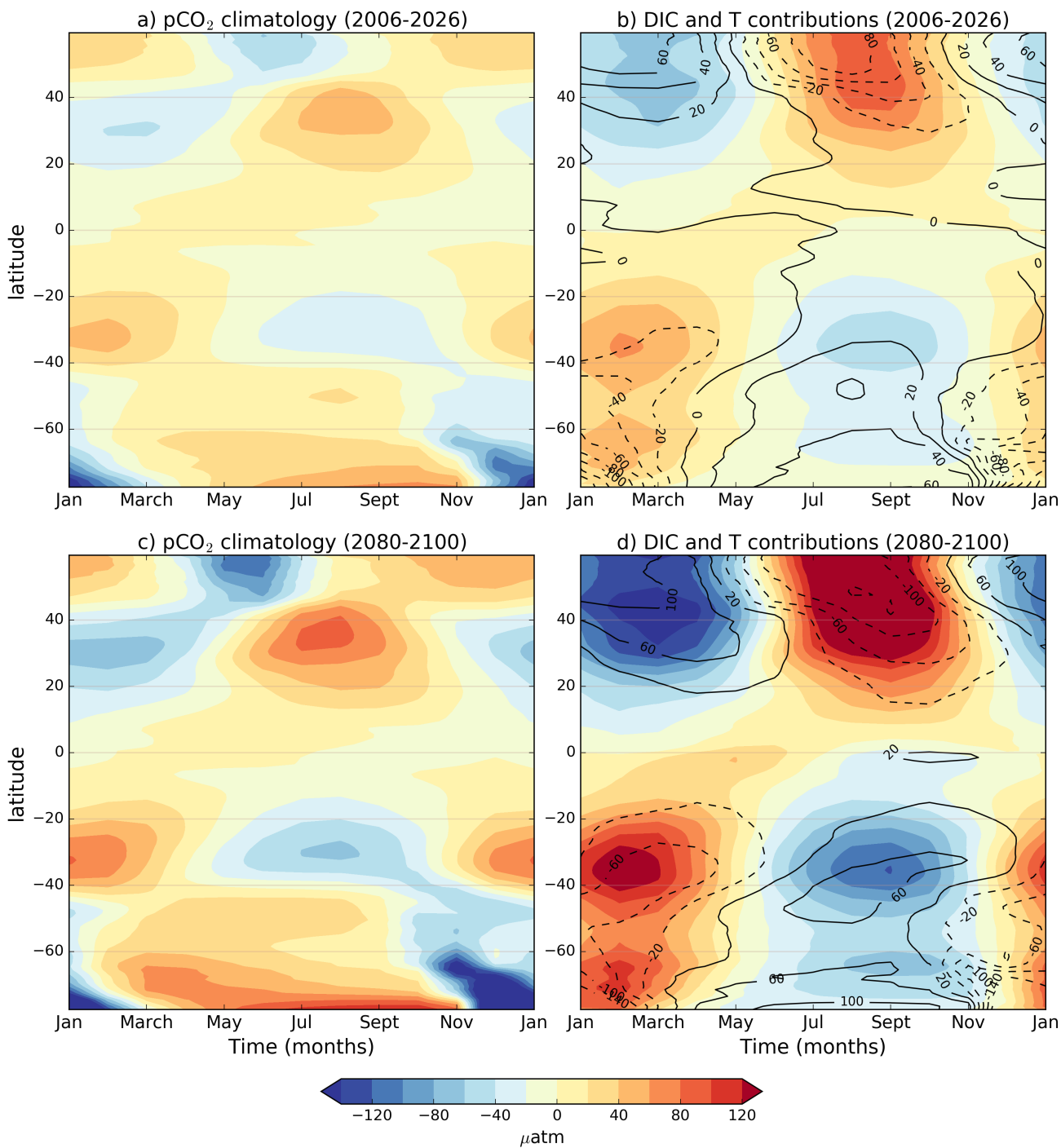


Figure S5. a) Ensemble zonal mean, zonal average of pCO₂ climatology and b) DIC contribution in color with overlying black contours of T contribution for 2006-2026 period. c) and d) same as a) and b) but for the 2080-2100 period.

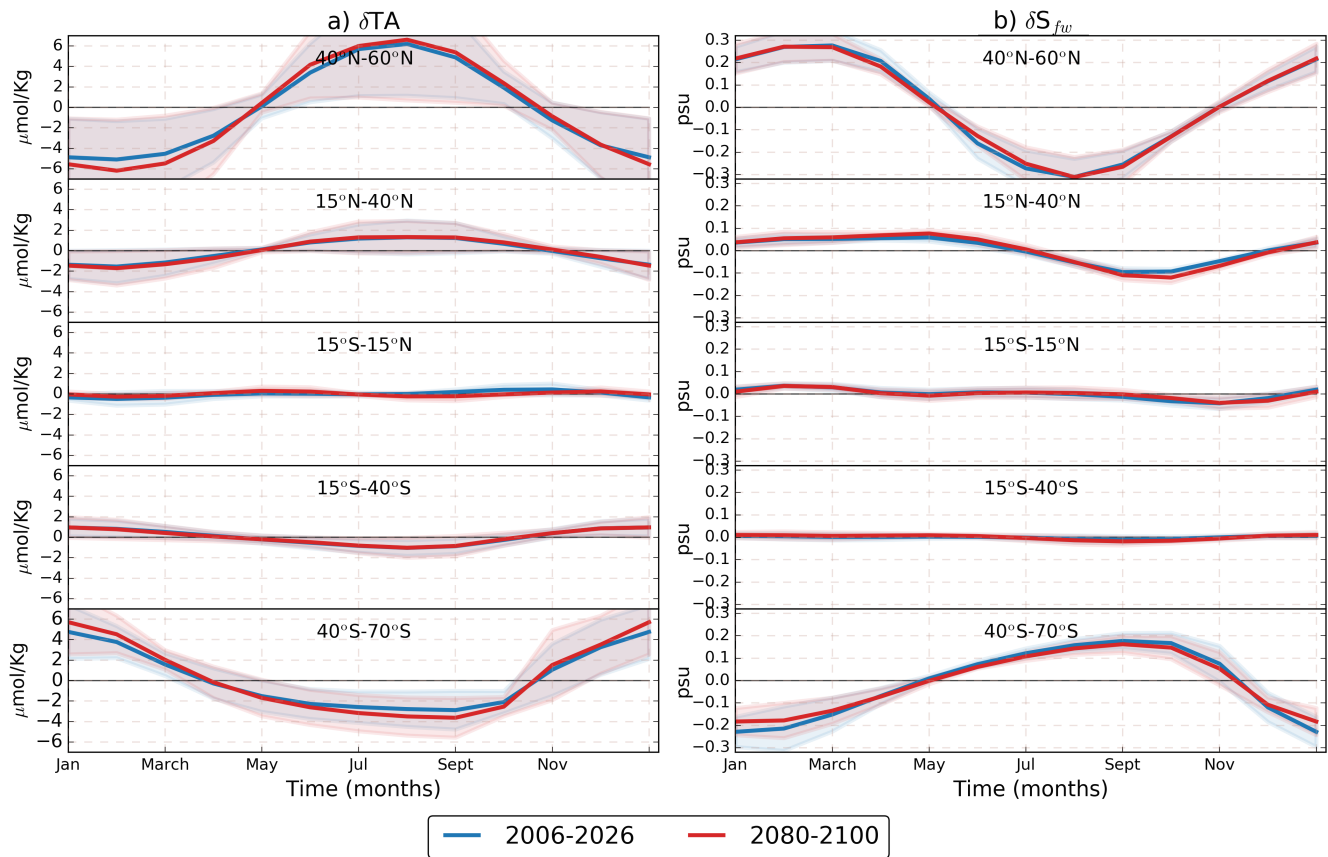


Figure S6. RCP8.5 ensemble zonal mean seasonal cycles: a) δTA_s and b) δS , for different latitudinal bands. Blue lines represent the 2006-2026 period, depicted for comparison with the 2080-2100 period shown by red lines. Different panels represent different latitudinal sections. δTA_s is projected to slightly increase in all the bands, while δS is projected to slightly decrease. The shading represents one standard deviation across the models.

References

- Dickson, A. G.: Thermodynamics of the dissociation of boric acid in synthetic seawater from 273.15 to 318.15 K, *Deep-Sea Research Part A. Oceanographic Research Papers*, 37, 755–766, 1990.
- 5 Egleston, E. S., Sabine, C. L., and Morel, F. M. M.: Revelle revisited: Buffer factors that quantify the response of ocean chemistry to changes in DIC and alkalinity, *Global Biogeochem. Cycles*, 24, GB1002, 2010.
- Landschützer, P., Gruber, N., and Bakker, D.: An updated observation-based global monthly gridded sea surface pCO₂ and air-sea CO₂ flux product from 1982 through 2015 and its monthly climatology (NCEI Accession 0160558). Version 2.2. NOAA National Centers for Environmental Information. Dataset. doi:10.7289/V5Z899N6, 2017.
- 10 Millero, F. J.: Thermodynamics of the carbon dioxide system in the oceans, *Geochemica et Cosmochemica Acta*, 59, 661–677, 1995.
- 10 Millero, F. J., Graham, T. B., Huang, F., Bustos-Serrano, H., and Pierrot, D.: Dissociation constants of carbonic acid in seawater as a function of salinity and temperature, *Marine Chemistry*, 100(1–2), 80–94, 2006.
- Takahashi, T., Sutherland, S. C., Sweeney, C., Poisson, A., Metzl, N., Tilbrook, B., Bates, N., Wanninkhof, R., Feely, R. A., Sabine, C. L., Olafsson, J., and Nojiri, Y.: Global sea-air CO₂ flux based on climatological surface ocean pCO₂, and seasonal biological and temperature effects, *Deep-Sea Research II*, 49, 1601–1623, 2002.
- 15 Takahashi, T., Sutherland, S. C., Chipman, D. W., Goddard, J. G., Newberger, T., and Sweeney, C.: Climatological Distributions of pH, pCO₂, Total CO₂, Alkalinity, and CaCO₃ Saturation in the Global Surface Ocean. ORNL/CDIAC-160, NDP-094. Carbon Dioxide Information Analysis Center, <https://doi.org/10.3334/CDIAC/OTG.NDP094>, 2014.